UNIVERSITY OF NAIROBI

DEPARTMENT OF ELECTRICAL AND INFORMATION ENGINEERING

Investigation of Natural Diatomite Sorption Properties for Application in Radioactive Waste Management

By

Nasio Cleophas Taula, B.Sc (Chemical and Process Engineering)

A research thesis submitted in partial fulfilment of the requirements for the award of Master of Science Degree in Nuclear Science and Technology, Department of Electrical and Information Engineering, University of Nairobi.

@ 2022

DECLARATION

I hereby declare that this thesis is my original work and has not been submitted elsewhere for examination or award of a degree at any other university. All sources and references used have been properly acknowledged and referenced in accordance with the University of Nairobi's requirements.

Nasio Cleophas Taula, S56/5964/2017

Signature: …… Date: 14th November, 2022

Supervisors' approval

This thesis has been submitted with our knowledge and approval as university supervisors:

1) Dr. Geoffrey O. Okeng'o
   Department of Physics,
   University of Nairobi
   gokengo@uonbi.ac.ke

   Signature: …… Date: ……15/11/2022……

2) Mr. Michael J. Mangala,
   Electrical and Information Engineering,
   University of Nairobi.
   michael.mangala@uonbi.ac.ke

   Signature: ……... Date: 15/11/2022……

DEDICATION

This thesis is dedicated to my parents for their steadfast support throughout my studies.

ACKNOWLEDGEMENTS

I am indebted to my supervisors; Dr. Geoffrey O. Okeng'o and Mr. Michael J. Mangala for their constant guidance during the entire process of thesis preparations. I would like to acknowledge the assistance received from Mr. Simion K. Bartilol, Chief Technologist, Institute of Nuclear Science & Technology, University of Nairobi and Mr. Shadrack O. Aluoch at Kenya Forestry Research Institute (KEFRI) for their guidance during laboratory sessions in this study.

TABLE OF CONTENTS

DECLARATION i

DEDICATION ii

ACKNOWLEDGEMENTS iii

LIST OF TABLES vii

LIST OF FIGURES viii

LIST OF ABBREVIATIONS AND ACRONYMS x

ABSTRACT xi

1 CHAPTER 1: INTRODUCTION 1

1.1 Background 1

1.2 Problem statement 2

1.3 Objectives 3

1.3.1 General objective 3

1.3.2 Specific objectives 3

1.4 Scope 4

2 CHAPTER 2: LITERATURE REVIEW 5

2.1 Characterization of Diatomite Minerals for Use as Adsorbents 5

2.1.1 Chemical composition of diatomite 5

2.1.2 Natural Radioactivity of Diatomite Minerals 7

2.1.3 Mineral Phase Composition of Diatomite Minerals 7

2.1.4 Particle size distribution of diatomite 11

2.1.5 Cation exchange capacity of diatomite 12

2.2 Diatomite and sorption of heavy metals from waste water streams 13

2.3 Diatomite and sorption of radionuclides for application in radioactive waste treatment 15

2.4 The influence of adsorption parameters on adsorption properties of diatomite 17

2.4.1 Influence of diatomite content on the sorption properties of diatomite 18

2.4.2 Variation of removal of ions with initial metallic concentration 19

2.4.3 Variation of removal of ions with the pH 20

2.4.4 Variation of ions removal with contact time 22

2.5 Synthesis, implication and identified knowledge gaps 24

3 CHAPTER 3: MATERIALS AND METHODS 26

3.1 Introduction 26

3.2 Chemical composition of Diatomite 26

3.3 Radioactivity characterization of Diatomite Samples 29

3.4 Determination of mineral phase composition of diatomite 27

3.5 Particle size analysis and measurements of diatomite 30

3.6 Determination of Cation Exchange Capacity of diatomite 32

3.6.1 The reagents used in determination of CEC of diatomite 32

3.6.2 Sodium acetate method of determining CEC of diatomite 32

3.6.3 Flame Photometric Determination of the Concentration of Sodium Displaced from the Diatomite Matrix 36

3.7 Determination of sorption capacity of Diatomite 36

3.7.1 Preparations of Simulated Radioactive liquid Waste Used in This Study 37

3.7.2 Variation of removal of ions with adsorbent content 37

3.7.3 Variation of removal of ions with initial metallic concentration 38

3.7.4 Variation of removal of ions with the pH 39

3.7.5 Variation of removal of ions with contact time 40

3.7.6 TXRF method used for determination of concentrations of Co, Zn and Ba 40

4 CHAPTER 4: RESULTS AND DISCUSSION 43

4.1 Introduction 43

4.2 Chemical composition of the diatomite samples 43

4.3 Radioactivity characterization of diatomite samples 46

4.4 The mineral phase composition of diatomite 44

4.5 The particle size distribution of the diatomite samples 46

4.6 Cation exchange capacity (CEC) of the diatomite samples 48

4.7 Sorption capacity of diatomite samples 51

4.7.1 Variation of removal of ions with sorbent concentration 51

4.7.2 Variation of removal of Co, Zn and Ba ions with the initial metallic concentration 55

4.7.3 Variation of removal of Co, Zn and Barium ions with contact time 66

4.7.4 The variation of removal efficiency of Co, Zn and Ba ions with pH 69

5 CHAPTER 5: CONCLUSIONS AND RECOMMENDATIONS 72

5.1 Conclusions 72

5.2 Recommendations 72

6 REFERENCES 74

LIST OF TABLES

Table 2.1:Chemical composition of diatomite from some of the selected studies 6

Table 2.2: The adsorption capacities of various adsorbents for cobalt uptake from water, Sheng et al (2012) 25

Table 4.1: Table of chemical composition of diatomite samples 43

Table 4.2: Activity concentration of 238U, 232Th, and 40K in diatomite samples from Kariandusi mining area, Kenya..... 46

Table 4.3: Particle size distribution of diatomite from Kariandusi Mining area, Kenya..... 47

Table 4.4: Intensity values for the calibration of flame photometer for determination of Na+ in samples..... 49

Table 4.5: Cation exchange capacity of diatomite from 4 trials 51

Table 4.6: The variation of removal of Co, Zn and Ba ions with the diatomite concentration52

Table 4.7: Comparison of Ionic radius and electronegativity of Zn, Co and Ba 53

Table 4.8: The variation of removal of Co, Zn and Ba ions with diatomite concentration 54

Table 4.9: The variation of sorption of Co, Zn and Ba ions from solution with initial metallic concentrations 57

Table 4.10: The variation of sorption of Co, Zn and Ba ions from solution with initial metallic concentrations 58

Table 4.11: The variation of the adsorption capacity of diatomite with initial metallic concentration of Co, Zn and Ba ions 62

Table 4.12: Variation of removal of Co, Zn and Barium ions with contact time 67

Table 4.13: The variation of amount of Co, Zn and Ba ions adsorbed on diatomite per unit mass of diatomite with contact time 67

Table 4.14: The variation of removal efficiency of Co, Zn and Ba ions with pH 70

Table 4.15: The variation of the amount of Co, Zn and Ba adsorbed on diatomite per unit mass of diatomite with the pH 70

LIST OF FIGURES

Figure 3.1: S1 Titan Brunker Model S1 Titan 600 series 600N 3187- MFG May 29, 2015, Mines and Geology Department, MOE, Kenya 27

Figure 3.2: Brunker D2 2 Gen Phaser Machine -Model D2 Phaser SSD 160 A 26-X1-A2DOB2B1, Mines and Geology, MoE , Kenya 28

Figure 3.3: Diatomite samples for Brunker D2 Phaser analysis, Mines and Geology, MoE Kenya 29

Figure 3.4: Rotap screen shaker for particle size measurements, Mines and Geology, MoE . 31

Figure 3.5: Edmund Buhler 7400 Tubingen mechanical shaker, at KEFRI, Kenya 33

Figure 3.6: Diatomite samples on MSE Centrifuge, KEFRI 34

Figure 3.7: Corning 400 Flame Photometer, Kenya Bureau of Standards, Kenya 35

Figure 3.8: BRUKER S2 PICOFOX TXRF available at Institute of Nuclear Science & Technology 41

Figure 4.1: Chemical composition of diatomite from Kariandusi Mining Area, Kenya 44

Figure 4.2: XRD pattern of diatomite sample from Kariandusi mining area, Kenya 45

Figure 4.3: Particle size distribution of diatomite from Kariandusi Mining area, Kenya 48

Figure 4.4: Calibration curve of concentration of Na against intensity of flame photometer readings 50

Figure 4.5: Variation of the removal of Ba, Zn and Co ions with diatomite concentration 53

Figure 4.6: Variation of removal of Ba, Zn and Co ions with of diatomite concentration 55

Figure 4.7: The variation of removal of Co, Zn and Ba ions from solution with initial metallic concentrations and diatomite content 59

Figure 4.8: The variation of removal efficiency of Co ions from solution with initial metallic concentrations and diatomite content 59

Figure 4.9: The variation of removal efficiency of Zn ions from solution with initial metallic concentrations and diatomite content 60

Figure 4.10: The variation of sorption efficiency of Ba ions from solution with initial metallic concentrations and diatomite content 60

Figure 4.11: The variation of the adsorption capacity of diatomite with initial metallic concentration of Co, Zn and Ba ions at a diatomite content of 2.0 g per 100 ml 63

Figure 4.12: The variation of the adsorption capacity of diatomite with initial metallic concentration of Co, Zn and Ba ions at a diatomite content of 2.5 g per 100 ml 64

Figure 4.13: The variation of the adsorption capacity of diatomite with initial metallic concentration of Co, Zn and Ba ions at a diatomite content of 3.0 g per 100 ml 65

Figure 4.14: Variation of removal of Co, Zn and Barium ions with contact time.....68

Figure 4.15: The variation of amount of Co, Zn and Ba ions adsorbed on diatomite per unit mass of diatomite with contact time 68

Figure 4.16: The variation of removal efficiency of Co, Zn and Ba ions with pH.....71

Figure 4.17: The variation of the amount of Co, Zn and Ba adsorbed on diatomite per unit mass of diatomite with the pH 71

LIST OF ABBREVIATIONS AND ACRONYMS

ADIL : African Diatomite Industries Limited

BET: Brunauer-Emmelt-Teller

C-D : Calcined diatomite

DF : Decontamination Factor

D-R : Dubinin–Radushkevich

Diat : Diatomite

EDXRF: Energy Dispersive X-Ray Fluorescence

EN : Electronegativity

FA : Fulvic acid

FC-D : Flux-calcined diatomite

FTIS: Fourier Transform Infrared Spectrophotometry

HA : Humic acid

HpGe : High Pure Germanium detector

HRS : Hours

ICP-OES: Inductively Coupled Plasma Optical Emission Spectrometry

IR: Infrared

KEBS : Kenya Bureau of Standards

KEFRI: Kenya Forestry Research Institute

MSD : Magnesium silicate/diatomite sorbent

MSE : Medical and Scientific Equipment

OECD : Organization for Economic Cooperation and Development

PZC : Point of Zero Charge

TXRF : Total X-ray Fluorescence

XRD : X-ray Diffraction

XRF : X-ray Fluorescence

ABSTRACT

This study has focused on characterizing diatomite samples from the Kariandusi Mining area, Kenya, for its possible application as a low-cost sorbent for radioactive ions of Ba, Co and Zn. The analysis of the chemical composition, mineral phases, radioactivity and particle size of diatomite was conducted using portable S1 Titan 600 series Bruker x-ray Fluorescence, gamma spectroscopy with the High Purity Germanium Spectrometer, Brunker D2 2 Gen Phaser XRD Machine and the Rotap screen shaker respectively. The sodium acetate method was used to determine the cation exchange capacity of diatomite. The sorption capacity of diatomite was investigated using prepared aqueous solutions containing stable ions of Ba, Zn and Co for the effect of sorbent concentration, initial metallic concentrations, sorption time and pH on the sorption capacity.

The chemical and mineral phase analysis of diatomite indicated that the diatomite was mainly composed of silica in the form of cristobalite, in agreement with the results on the typical composition of diatomite. The radiological characterization indicated that the radium equivalent activity of diatomite to be 77.96 ± 13.56 Bq/Kg, which was below the safe limit of 370 Bq/Kg recommended by the Organization for Economic Cooperation and Development (OECD). Particle size analysis show that 10% of particles had diameter less than 171 μm; 50% had a diameter less than 589 μm and while 90% of particles had less than 1523 μm. The particle size distribution may have affected the sorption capacity of diatomite by limiting the diffusion path length inside the sorbent. The diatomite's cation exchange capacity (CEC) was calculated as 7.94 ± 0.83 meq/100g compared to 9.8 meq/100g and 11.3 meq/100g obtained by Belousov et al (2019). The values of CEC vary because diatomite samples originating from different sources vary in pH, nature and quantity of clay minerals present. Analysis of the adsorption efficiency of diatomite for removal of Ba, Co and Zn ions showed that this increased with the diatomite concentration, contact time and pH because of increase in the number of sorption sites, continued interaction of the ions with the diatomite and enhanced physisorption. The sorption capacity was found to increase with the initial concentrations of ions because of the increase in the concentration gradient between the ions and the diatomite sorbent.

The highest removal efficiencies achieved in this study were 99.83%, 99.14% and 94.27% for Zn, Ba and Co respectively, showing that with a proper selection of sorption parameters highest removal efficiencies close to 100% can be achieved. This establishes that the diatomite samples from Kariandusi region have excellent sorption properties and can therefore be explored for radioactive waste management.

CHAPTER 1: INTRODUCTION

1.1 Background

The methods that are used for wastewater treatment include; reverse osmosis, ion-exchange or sorption, precipitation and coagulation. Using sorbents to remove radionuclides from radioactive liquid wastes has some advantages over the other methods; high selectivity and exhibits good stability against chemical, thermal and radiation (IAEA, 2001 & Shareef, 2009). The most notable merit of sorption is the potential to retain small quantities of substances from huge volumes of waste solutions (Aytas et al, 1999). Sorption is considered as the most feasible and affordable method in the treatment of liquid radioactive waste due to the variety of sorbent materials and ease of operation (Olatunji et al, 2018).

However, ion-exchange or sorption exhibits a few limitations. These limitations are; the mechanical strength and removal capacity of the most commonly used organic resins have been observed to deteriorate upon exposure to high temperature and radiation field, selectivity problems associated with removal of colloidal forms of Cs and Co from liquid wastes and the high cost of conventional sorbent materials (Rahman et al, 2011).

A review of the various methods used in the management of liquid radioactive wastes by Kim et al (2017), suggest the need to develop sorbents materials with higher ion exchange selectivity. To date, different materials with a variety of physical, chemical and structural characteristics have been tested for the capture of a variety of radionuclides from radioactive liquid wastes. However, few studies have been done on removal of Zn (Rahman et al, 2011).

In practice, the typical liquid radioactive wastes are composed of various radionuclides. ^{60}Co, ^{133}Ba and ^{65}Zn are some of the radionuclides typically present in liquid radioactive wastes (IAEA, 2003). Despite the fact that the actual liquid radioactive waste is composed of multiple radionuclides, most studied sorbent materials were either on single or bi-solute competitive sorption. This therefore, presents an opportunity for investigation on the selectivity and capacity of the local sorbents such as diatomite for multicomponent competitive sorption of the selected radionuclides from a simulated waste solution. The study is focused on evaluating the potential of diatomite for possible application in sorption of ^{60}Co, ^{133}Ba and ^{65}Zn from radioactive solutions.

Diatomite ($SiO_2.nH_2O$) is largely composed of silica. The structure of diatomite is made up of diatoms of typical size range of 10-200 mm with up to 80-90% voids (Galal Mors, 2010). Diatomite is a highly porous material with a low density and a large surface area. In the

industry, diatomite has found use as a filtration media for inorganic and organic chemicals and a sorbent for dealing with oil spillage.

Diatomite mineral is abundantly available in Kariandusi, Kenya and is mined by the African Diatomite Industries Limited (ADIL). The production capacity is currently at 30 tons per day; which translates to about 10,800 tons annually. Locally, diatomite from African Diatomite Industries Limited (ADIL) is used in the manufacture of; coatings, filter aids, absorbents, construction materials, organic grain preservatives, human food grade diatomaceous earth and food supplements (ADIL, n.d). The current market price of 10 kg of absorbent grade diatomite from ADIL goes at USD 6.

The sorption mechanisms proposed by scientists are; ion exchange, physical, chemisorption, coordination complexes and multicomponent sorption (Saint-Fort, 2018). These mechanisms are affected by the physical and chemical properties of the sorbent and aqueous solution containing the target ions. For instance, ion exchange will be affected by the cation exchange capacity of the sorbent and the competition between the target ions. Physical sorption would be affected by the surface charge on the sorbent and the pH of the solution containing the target ions. Chemical sorption is based on the chemical interaction of the target nuclide with the sorbent and is affected by the chemical composition of the sorbent. In multicomponent sorption, the contaminants with the lowest affinity for the active sites are desorbed from the sorbent and replaced by those with a higher affinity. Hence, evaluation of a new sorbent material involves characterization of its chemical, physical and sorption properties as well as investigation of the effect of sorption parameters.

This study sought to determine the physical and chemical properties of local diatomite samples from Kariandusi, Kenya, and evaluate the potential of diatomite as a candidate material for removal of ^{60}Co, ^{133}Ba and ^{65}Zn from liquid radioactive wastes.

1.2 Problem statement

Due to the increasing use of nuclear technologies in power generation, medicine, production industries and research, an increasing amount of radioactive waste is being generated from various sources, posing a serious threat and risk to health and safety of human and environment. Without proper treatment of radioactive waste, there is a huge risk of dissolved radionuclides migrating to the aquatic environment where their uptake by the plants or micro-organisms would see them find their way in human body through the interconnected food chains. The risk

of subjecting human beings and\or environment to undetected dangerous levels of radioactivity has been increasing. Exposure to high levels of radiation has the potential to cause death and increases the probability of diseases such as bone cancer, anemia, metabolic disorders and leukemia (Zhang et al, 2019).

Ion exchange or adsorption is one of the most well-established techniques used in management for liquid radioactive waste, but finding a cost effective and more efficient material remains a major challenge. In practice, the most commonly used materials in sorption or ion exchange for treatment of liquid radioactive wastes are known to exhibit poor mechanical strength and low removal capacity at high temperature. They have also been observed to deteriorate upon exposure to high radiation field (Rahman et al, 2011).

Studies of Co show evidence of selectivity problems when present in liquid wastes in colloidal forms. Cobalt has properties that are more like those of particles, rather than of ions. Consequently, the retention of Cobalt in colloidal form in the ion exchanger bed is limited and hence trapping colloidal forms of Co from liquid waste by conventional resins is difficult. However, a recent study by Ji-Min Kim and Chang-Lak Kim (2017) proposes the use of macro-porous materials whose porosity is higher enough to allow room for larger particles or ions to interact with the active sites within the beads.

There is need to evaluate the physical and chemical properties of local diatomite from Kariandusi mining area in Kenya as a potential low-cost material for sorption of Co, Zn and Ba for application in the management of radioactive liquid wastes.

1.3 Objectives

1.3.1 General objective

The main objective of the study was to evaluate the sorption properties of locally available natural diatomite materials from Kariandusi Mining Area for possible application in liquid radioactive waste management.

1.3.2 Specific objectives

The specific objectives of the study include:

a) To characterize diatomite samples from Kariandusi for use as sorbent
b) To establish the removal efficiency of selected ions by sorption on diatomite samples from Kariandusi for application of radioactive materials.

1.4 Scope

Diatomite is mined locally in Kenya and is abundantly available. However, its characterization and usage in the management of radioactive wastes have not been extensively studied. The aim of this study is to establish whether diatomite sorbent has the potential of use as sorbent material for radionuclides following its use in the treatment of heavy metal contaminated waste water streams. The scope of the study is limited to studying removal of Co, Zn and Ba by sorption on diatomite samples.

CHAPTER 2: LITERATURE REVIEW

2.1 Characterization of Diatomite Minerals for Use as Adsorbents

In general, characteristic properties of adsorbents such as; chemical composition, mineral phase composition, particle size and cation exchange enable us to fully gauge the potential of the sorbent's material for application use. The characteristics of the sorbents, as well, give us the insights on the type of modifications that can be applied on the sorbent to improve its selectivity towards sorption of certain target elements. The natural radioactivity of sorbents materials is an indication of their radioactive contamination prior to use.

This section presents findings on the various studies performed on the chemical composition, natural radioactivity, mineral phase composition, particle size distribution and cation exchange capacity of diatomite materials from different sources around the world.

2.1.1 Chemical composition of diatomite

The chemical composition of diatomite can be inferred from the origin and formation of diatomaceous rock. Diatomite is a mineral deposit originating from skeletal remains of diatomaceous algae. The principal constituent of diatomite is silica, a constituent of the diatom frustulae. In addition to silica, diatomite contains other components clays, salts, metal oxides and organic matter in variable amounts. The composition of the diatomite is affected by factors such as contact with the atmosphere, chemical precipitation and the environmental conditions at the mining facility. Besides, the level and nature of refining performed on the diatomite sample determines the final chemical composition. The findings from various selected studies on the chemical composition of diatomite are captured in table 2.1.

The data in table 2.1 on the chemical composition of diatomite from various authors indicates that the principal chemical constituent of diatomite is SiO_2 with varying smaller quantities of other oxides namely; Al_2O_3, Fe_2O_3, CaO, Na_2O, K_2O and MgO. Some of the diatomite samples shown in table 2.1 gave a SiO_2 concentration that was significantly higher than the others. For instance, the diatomite samples from Egypt and Mexico had Si_2 concentrations of 96.66 percent and 95.90 percent whereas the ones from Australia and Caldiran had 60.28 percent and 69.70 percent respectively. These differences may arise due to the variation

in the degree of purification. In addition, even in their raw form, the variation in chemical composition of diatomite is to be expected due to the fact that they are sourced from different geological sources.

Table 2.1:Chemical composition of diatomite from some of the selected studies

Constituent /Source	SiO_2 (%)	Al_2O_3 (%)	Fe_2O_3 (%)	CaO (%)	Na_2O (%)	K_2O (%)	MgO (%)	Other (%)	Reference
Egypt	96.66	3.06	-	-	-	-	-	0.28	Ibrahim et al (2013)
Germany	81.9	4.31	1.79	0.38	0.08	0.10	0.29	11.15	Belousov et al (2019)
Jordan	72.00	11.42	5.81	1.48	7.21			2.08	Aldegs et al 2001)
Australia	60.28	2.65	0.91	5.50		0.67		29.99	Meradi et al (2019)
Turkey	92.68	2.60		0.66	0.89	0.34	0.44	2.39	Yusani et al (2012)
Caldiran	69.70	11.50	4.40		0.80	1.40		12.20	Caliskan et al (2011)
Zhejiang	89.60	2.50	1.80	0.10	1.50			4.50	Sheng et al (2012)
Iran	89.20	4.10	1.50	0.50	1.20	0.63	0.30	2.57	Irani et al (2011)
Mexico	95.90	2.39	1.09	0.68	3.74	0.33	0.29		Flores et al (2013)
Serbia	79.72	10.20	2.51	0.05		1.31		6.21	Nenadovic et al (2015)
Birjand	73.20	11.60	1.50	1.30	1.00	0.50	1.50		Piri et al (2020)
China	84.2	6.51	5.23	1.32					Wu et al (2005)

Aktyubinsk	80.23	10.38		0.48	0.93	1.42	1.26		Mohamedbakr et al (2009)

2.1.2 Natural Radioactivity of Diatomite Minerals

The natural radioactivity of diatomite provides insight on whether it is contaminated with artificial radionuclides. It further indicates whether it is contaminated with significant quantities of the target metals. There are limited published studies on the natural radioactivity of diatomite.

Nenadovic et al (2015) analyzed the adsorption of cesium from radioactive solutions using natural diatomite from Rudovci, Serbia. The pysico-chemical characteristics of diatomite were determined and its adsorption properties studied. The natural radioactivity of diatomite sample was determined by the semiconductor HPGe spectrometer. The results showed that the diatomite sample did not have artificial radionuclides and that it did not contain $^{137}_{55}Cs$, which was the one of the reasons it was recommended as a suitable candidate material for the sorption of $^{137}_{55}Cs$ radioisotopes from nuclear radioactive waste streams.

2.1.3 Mineral Phase Composition of Diatomite Minerals

Diatomite falls under the silica sorbents and it has a wide variation in adsorption capacities. The differences in adsorption capacities may occur due to the differences in particle sizes or due to the type of treatment made by the manufacturer. Another factor that may influence the adsorption capacity of diatomite is the mineral phase composition which is dependent on the geographical source of occurrence. Belousov et al (2019) notes that the challenge of studying the sorption properties of natural minerals such as diatomite is the presence of contaminants such as smectite and illite. Since smectite and illite have a significant contribution towards the adsorption capacity, their presence in a natural sorbent needs to be known. The presence of minerals such as kaolinite with high sorption properties as well, have a notable effect on the sorption properties of natural sorbents. For instance, El Sayed (2018) notes that the presence of calcite in the Egyptian diatomite, a known sorbent material, contributed to the adsorption capacity of diatomite. The mineral phase composition of diatomite is therefore not only a key characteristic in describing the diatomite sorbent but also key when interpreting its adsorption

properties in comparison with other natural sorbents or other diatomite sorbents from various geographical sources. Let us now have a look at some of the findings on the mineral phase compositions of diatomite sorbents from various geographical sources as studied by several different authors.

Sheng et al (2008) analyzed the uptake of thorium (iv) on raw diatomite sample from Chengzhou county (Zhejiang province, China). According to the study, the diatomite sample was characterized and the role of influential variables on the sorption characteristics was evaluated. One of the key characteristics of diatomite that was determined was its mineral phase composition. The diatomite sample was analyzed for phase identification by XRD on CuK_{α} radiation with a Rigaku X-ray diffractometer. From the study results, the diffraction spectrum showed that the sample of diatomite consisted principally of silica (SiO_2) and minor quantities Fe_2O_3, Al_2O_3, CaO and Na_2O. The x-ray diffraction spectrum indicated that a non-crystalline phase was present and was associated with the glass formation of silica.

Caliskan et al (2011) investigated the uptake of zinc (II) by raw diatomite from the Caldran region of Lake Basio Anatolia (Turkey) and the effect of the modification of diatomite with an oxide of manganese. The diatomite was characterized and its kinetic and equilibrium adsorption properties investigated. The mineral phase composition was conducted using the method of X-ray powder diffraction and the results showed that the sample of diatomite was predominantly composed of silica (SiO_2) with minor quantities K_2O, Fe_2O_3, Na_2O, Al_2O_3, and TiO_2. The non-crystalline band was attributed to the glass formation of SiO_2.

Yusani et al (2012) conducted an investigation on the uptake of thorium (IV) on calcined and flux-calcined diatomite from Turkey. The diatomite sample was characterized and its adsorption properties studied under varying operating conditions. Mineral phase identification was conducted by X-ray diffraction method using Phillips X'Pert Pro and Fourier Transform Infrared Spectroscopy. The XRD spectrum indicated that the major peaks of the calcined sample of diatomite corresponded to tridymite, cristobalite and small amount of quartz.

Flores-Cano et al (2013) performed a study on the mechanism uptake of heavy metals on the diatomite (from Jalisco, Mexico) and the influence of the operating variables. The diatomite sample was characterized and its sorption properties analysed under varying conditions of pH and temperature. On characterization, the chemical composition, texture, morphology, cation exchange capacity, mineral phase composition and surface charge distribution were studied. The mineral phase composition was determined by the XRD technique. The study results

showed that apart from the presence of silica in the form of cristobalite and quartz, a non-crystalline band was noted and was associated with glass formation of silica.

Nenadovic et al (2015) conducted a study on the uptake of cesium from radioactive solutions using natural diatomite sample from Rudovci, Serbia. The characteristics of the diatomite sample were determined by Scanning Electron Microscope (SEM) and X-rya diffraction methods. The XRD anaylsis indicated that the main mineral constituents were quartz, muscovite, kaolin and enstatite. The diffraction results revealed that the sample of diatomite consisted principally of silica (SiO_2) with small quantities of $CaO, Al_2O_3, Na_2O,$ and Fe_2O_3. The SEM results indicated that the diatomite sample was highly porous and with large volume. The high porosity and large void volume were one of the key reasons that the diatomite sample was selected for sorption of cesium.

Lu et al (2017) studied the uptake of uranium (VI) by the magnesium-silicate-diatomite. The raw and the treated diatomite were characterized, equilibrated with uranium (VI) and the role of ionic strength and pH investigated. The raw and the treated diatomite were characterized by determining its morphology, mineral phase identification and specific surface area using the Brunauer-Emmett-Telle (BET), scanning electron microscope and X-ray diffraction techniques respectively. From the X-ray diffraction studies, the diffractions patterns of diatomite indicated that the peaks obtained at diffraction angle of 2θ corresponded to the crystal planes of Si_2.

El Sayed (2018) conducted an investigation on the uptake of heavy metals by the Egyptian diatomite. The diatomite sample was characterized and its sorption properties studied under the influence if contact time, pH and diatomite content. Characterization involved determination of diatomite morphology by done by scanning electron microscope and identification of mineral phases by X-ray diffraction method. On XRD analysis, the spectrum and peaks obtained at 2θ diffraction angles indicated that the diatomite sample contained calcite, quartz and clay minerals. It was found that the presence of calcite, a known sorbent material, contributed to the adsorption capacity of diatomite.

Sandhaya et al (2018) studied the use of diatomite sample from Australia as a source of silicon fertilizer for the South Indiana rice. The diatomite sample was characterized by describing its morphology using scanning electron microscope, determination of its chemical composition using inductively coupled plasma optical emission spectrometer and identification of its mineral phase composition using X-ray diffraction technique. From the XRD studies, the XRD

spectrum and the peaks at the 2θ diffraction angles indicated predominance of quartz, kaolinite and smectite in the diatomite sample.

Belousov et al (2019) studied the uptake of cesium by glauconite, bentonite, zeolite and diatomite from Munsingen, Germany. The sorbents were characterized and sorption properties studied by contacting it with radioactive cesium solution. XRF, XRD, IR, FTIR and SEM techniques were employed to determine the characteristics of the sorbents. From the XRD study, the XRD spectrum and the peaks at the 2θ diffraction angles showed that the diatomite sample was mainly consisted of diatom shells with opal structure with a weight percentage of 80.8%. The results further indicated that the diatomite sample contained 9.9 percent of smectite, 9.0 percent of kaolinite and 0.3 percent of quartz. The presence of sepiolite/pyrophyllite admixture was noted but was not quantified.

Borges et al (2019) study on diatomite involved treating diatomite from Rio Grande do Norte, Northeast of Brazil with microemulsion and evaluating its adsorption properties with regard to uptake of metal cations from solutions. The characteristics of the diatomite samples were determined by x-ray fluorescence, scanning electron microscopy, thermogravimetry, FTIS, X-ray diffraction and BET method. From the XRD study, it was shown that even though the diatomite sample was predominantly amorphous, crystalline peaks associated with Kaolinite and Quartz were present.

Meradi et al (2019) study focused on characterization of Algerian diatomite sample from Sig region. The diatomite sample's morphology was characterized by scanning electron microscope, its chemical composition by the X-ray Fluorescence, mineral phases identification by X-ray diffraction method and particle size analysis in an air vacuum sieve. From the XRD analysis, the spectrum and the peaks at 2θ diffraction angles indicated that the diatomite sample was principally composed of calcite, quartz and ankerite.

In general, the studies on the mineral phase composition of diatomite indicate that the mineral phases of diatomite are predominated with polymorphs of silica, most notably quartz, opal and cristobalite. It is worth noting that apart from the consistency reported by several authors on the presence of quartz, opal and cristobalite, the other components of diatomite mineral vary from one geographical source to another. While several authors have presented the mineral phase composition of their respective diatomite samples, most of them have not explained how the individual mineral phase components influence the adsorption properties of diatomite. In addition, some authors used raw diatomite, others subjected it to purification prior usage while

others sourced their diatomite from manufacturers. As to what extent these differences affect the mineral phase composition and the adsorption properties of diatomite is a subject that requires closer scrutiny.

2.1.4 Particle size distribution of diatomite

The particle size of a sorbent material can be correlated to its surface area. It is known that adsorption is phenomenon that is dependent upon the specific surface area of the sorbent and therefore it is important to specify the particle size of an adsorbent as it affects the surface area of the sorbent. While the use of sorbents with particle size in the nanometer range will realize higher adsorption capacities, the difficulty of regeneration of the adsorption column due to large pressure drops is a critical factor to be considered in selection of the optimum particle size. Let us now have a look at what several authors have done on the diatomite particle size in their studies.

Caliskan et al (2011) conducted a study on the uptake of zinc (II) by diatomite from the Caldran region of Lake Basio Anatolia (Turkey) and the effect on adsorption properties of diatomite when it was modified with an oxide of manganese. The diatomite was characterized and its kinetic and equilibrium adsorption properties investigated. On the study about the particle size distribution, the micrographs of diatomaceous earth and modified diatomite showed that the diatomite sample had particle size distribution of 0.005-0.025 mm.

Nenadovic et al (2015) conducted an investigation on the uptake of cesium from radioactive solutions using natural diatomite from Rudovci, Serbia. The diatomite was characterized and its efficiency evaluated for the upatke of cesium from radioactive liquid wastes. One of the physico-chemical characteristics studied was the particle size distribution of the diatomite sample used in the study. The results showed that 10% of particles had a diameter less than 3.074 μm, 50% of particles had a diameter of 4.963 μm, while 90% of particles were less than $11.078 \mu m$.

Meradi et al (2019) study focused on characterization of Algerian diatomite sample from Sig region. The diatomite sample's morphology was characterized by scanning electron microscope, its chemical composition by the X-ray Fluorescence, mineral phases identification by X-ray diffraction method and particle size analysis in an air vacuum sieve. On particle size analysis, Meradi et al (2019) conducted a granulometric analysis of the diatomite sample and

found that more than 80% of the mass of the diatomite was composed of grains of 90 to 200 microns.

Most of the published studies on the adsorption properties of diatomite for metal cations have not indicated how the particle size used in their respective studies was arrived at. Neither has the influence of the size of particles on the adsorption properties of diatomite been extensively investigated. Adsorption being a surface phenomenon, you would expect that the researchers will focus significant effort in size reduction. However, it is worth noting that diatomite is a porous adsorbent with pores which are much smaller than the particle size and contributes more to the surface area. Kumar et al (2019) notes that carrying out size reduction on porous sorbents does not result in significant improvement in the surface area since most of the surface area of porous sorbents arise from pores smaller than 50 nm, a size that is much smaller than the particle size of the sorbents. Hence there is tendency of the research leaning on studying the effect of pore size distribution rather than particle size distribution.

2.1.5 Cation exchange capacity of diatomite

The cation exchange capacity of a sorbent provides insight about the number of negative sites in the sorbet matrix that can be exchanged with cations per 100g of the sorbent. It is a measure of the adsorption capacity of a sorbent if the target metals are adsorbed by the mechanism of cation exchange. Several authors have investigated the cation exchange capacity of diatomite samples from various sources and varying results have been obtained depending on the method used and the respective chemical composition of the diatomite under study. It is worth noting that, only a few authors determined the cation exchange capacity of diatomite in their adsorption studies.

Flores-Cano et al (2013) analyzed the uptake of heavy metals by diatomite. The study was based on the mechanism of adsorption and the influence of the operating variables. One of the important characteristics of diatomite studied was the cation exchange capacity (CEC). To study the influence of cation exchange capacity, the diatomite sample (Jalisco, Mexico) was analyzed for CEC using the method of Ming and Dixon (1987) and it was found that the cation exchange capacity of the diatomite was 1.27 meq/g. Based on the concentration of Na_2O in the diatomite, the theoretical value of CEC for diatomite was determined to be 1.21 meq/g which was close to the experimental value obtained.

Nenadovic et al (2015) investigated the uptake of cesium from radioactive solutions using natural diatomite from Rudovci, Serbia. The characteristics of the diatomite sample were

determined by X-ray diffraction and Scanning Electron Microscope methods while the cation exchange capacity was done by the standard procedure (EPA, 1986) used for calcareous and noncalcareous soils. Sorption studies analysed the role of pH and initial concentration of cesium. On the cation exchange capacity, the it was found that the CEC value of diatomite was 50 meq/100g.

Belousov et al (2019) studied the uptake of cesium by glauconite, bentonite, zeolite and diatomite from Munsingen, Germany. The sorbents were characterized and sorption properties studied by contacting it with radioactive cesium solution. XRF, XRD, IR, FTIR and SEM techniques were employed in determining the characteristics of the sorbents. The cation exchange capacities for the sorbents were determined using methylene blue method, ammonium chloride solution and the Mehlich's method. For diatomite, the CEC analysis was determined using adsorption of MB and by the Mehlich's method giving close results of 9.8 and 11.3 meq/100 g respectively.

Piri et al (2020) studied immobilization of toxic heavy metals namely; lead, cadmium, zinc and copper in contaminated soil by application of diatomite sample from Birjand mine, Iran. The chemical composition, morphology and microstructural characteristics of the diatomite sample were measured by XRF and SEM. Piri et al (2020) estimated the CEC value of the diatomite sample as 80 cmol/kg.

The studies on cation exchange capacity indicate that CEC values of diatomite vary from one diatomite source to another. This is expected since the various diatomite samples used in the studies do not have identical chemical composition, mineral phase composition nor do they originate from the same geographical source. In addition, it is difficult to make any meaningful comparisons, since not all the diatomite samples from various authors were subjected to the same mode of preparation. It remains unclear whether the differences in the methods selected for determination of cation exchange capacities could have contributed to the huge variations in cation exchange capacities obtained by various authors.

2.2 Diatomite and sorption of heavy metals from waste water streams

Accumulation of heavy metals in water bodies remains as serious threat to the health of human and aquatic level. Environmental regulatory authorities continue to impose stiffer regulations that require reduction in emission of toxic elements in water bodies. The use of natural sorbents such as diatomite has continued to receive attention as they are not only affordable but also environment friendly. Several studies have been conducted on the application of diatomite for

adsorption of heavy metals from solutions for application in sorption of heavy metals from waste water streams. Some of the work done on the application of diatomite for sorption of heavy metals from contaminated liquid streams is presented next.

Caliskan et al (2011) conducted a study on the uptake of zinc (II) on diatomite sample from the Caldran region of Lake Basio Anatolia (Turkey) and evaluated the impact on the adsorption properties of diatomite when it was modified with an oxide of manganese. The diatomite was characterized and its kinetic and equilibrium adsorption properties investigated. According to the study results of adsorption isotherms, it was determined that Freundlich, Langmuir and D-R adsorption isotherms provided a good fit. The data obtained sorption study was seen to fit properly on Langmuir, Freundlich and D-R adsorption isotherms. The process of adsorption of zinc (II) on the diatomite sample was physical and spontaneous.

Irani et al (2011) investigated the uptake of lead on Iranian clays namely; diatomite, dolomite and perlite. According to the study, the sorption capacity was found to be greater for diatomite sorbent than that for dolomite or perlite. On the optimum sorption parameters, the study indicated that the lead adsorption was optimum when the temperature was maintained at 45°C and the pH kept at 6.

The uptake of heavy metals on the Mexican diatomite was studied by Flores-Cano et al (2013). The study sought to explain the adsorption mechanisms involved in the uptake of zinc, cadmium, chromium and lead on the diatomite as well as the role played by the nature of the target metal, solution pH and temperature on adsorption properties of diatomite for the target metal cations. As per the results obtained in the study, the highest adsorption capacities observed for Cr (III), Pb (II), Zn (II), and Cd (II) were 0.162, 0.169, 0.232 and 0.734 respectively. On the mechanisms of adsorption, the adsorption of cadmium was found to be principally governed by chemisorption while ion exchange taking up about 10 to 50 percent.

Ibrahim et al. (2013) studied the uptake of lead (II), cadmium (II), nickel (II), copper (II) and zinc (II) on three types of Egyptian diatomite: refined, natural, and classified diatomite. The results showed that the equilibrium for Cadmium and Zinc was reached after 15 minutes, while the equilibrium for copper was reached after 30 minutes. Equilibrium was reached after 60 minutes for Nickel and Lead. The optimum metallic concentration and pH obtained were 9.0 g/l and 4.7 respectively. According to the findings, the refined diatomite was the most efficient, with a selectivity sequence of $\mathrm{Pb}^{2+} > C\mathrm{d}^{2+} > Z\mathrm{n}^{2+} > C\mathrm{u}^{2+} > N\mathrm{i}^{2+}$.

The study on the uptake of lead (II) ions by diatomite sample from Çankırı-Çerkeş Basin of Turkey was conducted by Salman et al (2016). From the study, the highest value observed for the uptake of lead (II) ions on diatomite sorbent was 26 mg\g. On the study concerning the adsorption model, the results showed that the Freundlich model provided a good fit to characterize the uptake of lead (II) ions on the diatomite sample from Çankırı-Çerkeş Basin of Turkey

ElSayed (2018) investigated the adsorption of various metallic ions on natural diatomite from El-Fayoum, Egypt. The role of pH, sorption time and adsorbent content on the capacity of diatomite to adsorb the target metallic ions was studied. According to the study, the maximum uptake of heavy metal cations was observed when the pH was set to 4 and that increasing adsorbent content and contact time positively influenced metal ion removal.

After treating diatomite from Rio Grande do Norte, Northeast of Brazil with a microemulsion, Borges et al (2019) studied its uptake for metallic ions. The diatomite samples were characterized by x-ray fluorescence, scanning electron microscopy, thermogravimetry, FTIS, X-ray diffraction and BET method. The results on the effect of the treatment with a microemulsion showed that the ethoxylate groups in the microemulsion-treated-diatomite were critical in improving the sorption capacity for the Fe^{3+}, Pb^{2+} and Cr^{6+} ions.

2.3 Diatomite and sorption of radionuclides for application in radioactive waste treatment

With the use of nuclear techniques in medicine, manufacturing industry, research and power generation increasing, so is the risk of contamination of water bodies with injurious levels of radioactive wastes. A common problem in treatment and handling of radioactive liquid waste is the sorption and immobilization of harmful radionuclides from waste water drainage systems. Low-cost natural sorbents can be used to solve this problem. Diatomite is one of the low-cost naturally occurring sorbent. The use of diatomite for waste treatment has received a significant attention in the recent past. We can now look at some work done on the application of diatomite for treatment of radioactive wastes.

To start with, (Aytas et al, (1999)) conducted a study on the uptake of uranium on diatomite earth (Kieselguhr). Aytas et al studied the role of temperature, pH, initial concentration of uranium and contact time on the adsorption properties of diatomite for uranium. From the study results, the highest removal percentage of Uranium was 77% and was achieved at a pH of 5.0

In another study, Osmanlioglu (Osmanlioglu, 2007) treated radioactive liquid containing Cesium-137, Cesium-134 and Cobalt-60 with the natural Turkish diatomite and found that its radioactivity had dropped from the $2.60\ Bq/ml\ to\ below\ 0.40\ Bq/ml$. This reveals that, treatment of the radioactive solution with diatomite resulted in around 85% reduction in the radioactivity of the initial solution.

A study on the uptake of Th (IV) on raw diatomite from Zhejiang, China was conducted by Sheng et al (2008). As per the study results, the sorption process was not only rapid but also endothermic. The study further indicated that the capacity of diatomite to adsorb Th (IV) was sufficient for application on large volumes of aqueous waste containing Th (IV).

Yusan et al (2012) carried out an investigation on the uptake of thorium (IV) on diatomite samples that were either treated by calcination or flux-calcination from Turkey. The diatomite sample was characterized and its adsorption properties studied by investigating the role of operating parameters namely; initial metallic concentration, pH, temperature and contact time. From the investigation on sorption properties, the results showed that the uptake of Th (IV) on diatomite was very effective, fast and depended on temperature, initial Th (IV) concentration and the pH.

Sheng et al (2012) characterized diatomite from Zhejiang, China and evaluated its potential application for sorption of radiocobalt. According to the study, the sorption of cobalt was influenced by ionic strength as the pH was lowered while the effect of ionic strength was not evident at high values of pH. The increase in uptake of Co (II) at low pH and the reduced adsorption at high pH was associated with the presence of HA/FA. The data obtained on the adsorption thermodynamics of Co (II) on the diatomite showed that the uptake of Co (II) on diatomite was rapid and endothermic

In his other study, Osmanlioglu (2015) investigated the effect of increasing the amount of diatomite in the diatomite-cement matrix on its effectiveness to immobilize radioactive borate liquid waste. According to the results obtained from the study, the increase in the quantities of diatomite in the cement matrix was found to enhance the isolation effectiveness of the solidified waste.

Nenadovic et al. (2015) study was based on the uptake of cesium from radioactive aqueous solutions on natural diatomite from Rudovci, Serbia. The characteristics of the diatomite sorbent were determined by X-ray diffraction and Scanning Electron Microscope methods while the cation exchange capacity was done by the standard procedure (EPA, 1986) used for

calcareous and noncalcareous soils. Sorption studies evaluated the role of pH and initial concentration of cesium. According to the study, the initial concentration of Cs was found to heavily influence its adsorption characteristics on diatomite. From the kinetic experiments, the study noted that the process of adsorption of Cs on diatomite occurred in two steps that involved fast adsorption Cs ion on the surface of diatomite and subsequent diffusion of Cs to the interior of the adsorbent.

The adsorption of uranium (VI) on magnesium-silicate-diatomite was investigated by Lu et al (2016). The raw and the treated diatomite were characterized, equilibrated with uranium (VI) and the role of ionic strength and pH investigated. The raw and the treated diatomite were characterized by determining its morphology, mineral phase identification and specific surface area using the Brunauer-Emmett-Telle, scanning electron microscope and X-ray diffraction techniques respectively. As per the study, the maximum adsorption capacity of 31.53 milligrams of U (VI) per gram of magnesium silicate\diatomite sorbent observed at a pH of 5.0 and temperature of 293 K was greater than that observed for other natural clay minerals. The study indicated that magnesium silicate\diatomite sorbent exhibited adequate sorption capacity for capture and retention of radionuclides from radioactive waste streams.

The results from the work done on the application of diatomite for sorption of metal contaminants in their solutions, indicate that diatomite has performed significantly well. However, some of the studies have been conducted using target contaminants in their stable form rather than in their radioactive form. It remains to be seen whether the results obtained with stable contaminants can be replicated if the contaminants are used in their radioactive form

2.4 The influence of adsorption parameters on adsorption properties of diatomite

The knowledge of the effect operating parameters on the sorption properties of diatomite is important in determining the optimum operating conditions for use in applications, as well as in enabling compare findings from different studies carried out under different operating conditions. Some of the important parameters that have been studied by various authors that are of importance to this study include; the influence of diatomite content, influence of initial metallic concentration, role of pH and role of contact time. The findings from selected studies on the effect of these parameters are presented next in the sections.

2.4.1 Influence of diatomite content on the sorption properties of diatomite

An increase in the diatomite content will increase the number of binding spaces on the sorbent for uptake of target metals. Therefore, the removal efficiency of a sorbent is enhanced when its content per volume of the simulated solution is increased. On the adsorption capacity, however; an increase in the diatomite content does not necessarily translate to an enhancement in the adsorption capacity. Adsorption capacity is commonly expressed in terms of the mass or moles adsorbed per unit mass of the sorbent and may increase, decrease or remain constant if the sorbent content is increased depending on the utilization factor of the available sorption sites. The diatomite content also referred to as the "dose" in some studies, is an important parameter in evaluating the potential of the candidate sorbent material. Let us now look at some of the studies conducted on the influence of diatomite content and their respective findings.

The study on application of diatomite (Zhejiang province, China) for removal of thorium from solutions was conducted by Sheng et al (2008). The diatomite sample was characterized and the effect of operating conditions (namely; pH, temperature, contact time and ionic strength) on the adsorption properties evaluated. On the role of the diatomite content per unit volume of solution on the adsorption of Th (IV), Sheng et al (2008) indicated that the removal efficiency of thorium (IV) was enhanced as diatomite content was increased up to 0.25 g\L. As the diatomite dose was increased beyond 0.25 g\L, the increase in percentage adsorption occurred at a diminishing rate.

So as to determine the role of diatomite content on the sorption of cadmium (II), copper (II), lead (II), nickel (II), and zinc (II) by Egyptian diatomite, Ibrahim et al (2013) varied the amounts of diatomite content from 1 to 10 g/L while maintaining shaking time and metal concentration constant at 120 min and 50 mg/L, respectively. As per the study results, the percentage adsorption was enhanced as the adsorbent content was increased and reached equilibrium at 9 g/L, with percentage adsorption reaching 75.6 percent for lead (II), 54.8 percent for cadmium (II), 30.4 percent for Copper (II), 29.4 percent for Nickel (II), and 39.7 percent for Zinc (II).

Salman et al (2016) studied uptake of lead (II) ions by the diatomite sample from Turkey. The study focused on the mechanism of sorption, adsorption isotherm, kinetic studies and the role of pH, contact time and adsorbent content. To investigate the role of adsorbent content on the sorption of lead by diatomite, Salman et al (2016) varied the diatomite content in the range (2 to 10 g/l). According to the study, the uptake of Pb (II) increased with increasing diatomite

content for contents ranging from 2g/l to 4g/l, but not significantly for adsorbent contents greater than 4g/l.

ElSayed (2018) studied the influence of diatomite content on the uptake of heavy metals. The results showed that by increasing the diatomite content from 0.5 g/L to 2 g/L, the percentage uptake of heavy metals was enhanced from 55.2 percent to 99.7 percent. According to the study, as diatomite content was increased, so did the number of adsorption sites in contact with the metal ions. As a result, lower diatomite concentrations reached surface saturation faster than higher diatomite concentrations.

2.4.2 Variation of removal of ions with initial metallic concentration

Caliskan et al (2011) carried out an investigation on the uptake of zinc (II) on diatomite and manganese-oxide modified diatomite from the Caldran region of Lake Basio Anatolia (Turkey). The diatomite was characterized and its kinetic and equilibrium sorption properties evaluated. The investigation examined the variation of Zn (II) ions removal with pH, contact time, initial concentration and temperature. On the variation of initial metallic concentration, the uptake of Zn (II) on modified and natural diatomite was found to increase linearly as the initial concentrations of Zn (II) was increased.

Irani et al (2011) study involved investigation of the uptake of lead on Iranian clays namely; diatomite, dolomite and perlite. Using diatomite, dolomite and perlite as sorbents, the variation of lead (II) ions removal with pH, contact time and the initial metallic concentration were studied. On the variation of initial concentration, the study found out that, when the initial concentration of lead (II) ions was raised, the number of lead ions in contact with active sites of sorbents increased, thereby enhancing adsorption. However, as when the initial concentration of lead was enhanced further, the active sites on the diatomite sorbent were saturated and the adsorption capacity approached a constant value.

Yusani et al (2012) conducted an investigation on the uptake of thorium (IV) on diatomite samples from Turkey which were first either treated by calcination or by flux-calcination. The diatomite sample was characterized and its adsorption properties evaluated at different operating levels of pH, starting metallic concentration, temperature and contact time. The effect of varying the initial metallic concentration on the sorption of Thorium (IV) by Turkish diatomite was investigated in the range 25 to 50 mg\L. According to the study, the uptake of thorium (IV) on both calcined and flux-calcined diatomite was enhanced when the starting concentration of thorium (IV) was raised from 25 to 50 mg\L.

Nenadovic et al (2015) carried out a study on the uptake of cesium from radioactive solutions using natural diatomite from Rudovci, Serbia. The mineral phase composition, morphology and microstructural characteristics of the diatomite sample were determined by X-ray diffraction and Scanning Electron Microscope methods while the cation exchange capacity was done by the standard procedure (EPA, 1986) used for calcareous and noncalcareous soils. On sorption studies Nenadovic et al (2015) analyzed the variation of the immobilization effect of diatomite with the initial cesium concentration in acidic and alkaline medias. According to the study results, the efficiency of immobilization was enhanced as the initial concentration of cesium was reduced. In comparison to acidic media, the effect of immobilization in alkaline media was greater and less influenced by the initial Cs concentration.

2.4.3 Variation of removal of ions with the pH

Sheng et al (2008) investigated the uptake of thorium (iv) on the diatomite (Zhejiang province, China) and examined the change caused by varying the operating conditions namely; the temperature, pH, contact time and ionic strength. On the influence of varying pH on the sorption of Th (IV) by diatomite, Sheng et al indicated that the uptake of Th (IV) grew rapidly as the pH was raised for pH<4, but then remained constant as pH was raised beyond a pH of 4. The removal efficiency approached 100% for pH<4 and the removal of Thorium was not associated with precipitation. The study indicated that precipitation of Thorium on diatomite surfaces occurred at a $pH \sim 4$.

Irani et al (2011) carried out analysis of the uptake of lead on Iranian clays namely; diatomite, dolomite and perlite. The effect of varying pH, contact time and the initial metallic concentration on the adsorption properties of diatomite, dolomite and perlite for lead were studied. On the effect of varying pH, Irani et al observed that the lead sorption grew when the pH of the aqueous solution was raised from 2 to 6. The sorption of lead by diatomite achieved a peak value at pH 6, but it was observed to decrease at pH values higher than 6.

In order to evaluate the variation of adsorption of Co (II) with initial pH on the Chinese diatomite, Sheng et al (2012) varied the pH from 2.0 to 12 while keeping the temperature at 293 K. It was found that the sorption of Co (II) on diatomite increased gradually as the pH was increased from 2.0 to 5.0, then rapidly enhanced as the pH was raised from 5.0 to 8.0, while it maintained a high level of approximately 90% when the pH was increased beyond 8.0.

Yusani et al (2012) conducted an investigation on the uptake of thorium (IV) on calcined and flux-calcined diatomite from Turkey. The diatomite sample was characterized and the changes in its adsorption properties determined at different operating levels of contact time, pH, starting metallic concentration and temperature. On the effect of variation of pH on the uptake of Th (IV) on Turkish calcined and flux-calcined diatomite, the study results showed that the maximum adsorption percentage of 99 percent was observed for both calcined and flux calcined diatomite when the pH was set at 4.0.

In their study on the effect of pH on uptake of cadmium (II), copper (II), lead (II), nickel (II), and zinc (II) by Egyptian diatomite, Ibrahim et al (2013) observed a notable rise in the uptake efficiency of metal ions when the pH was increased from 1.5 to 4.7 but becmae level for a pH range of 4.7 to 5.5. It was found that when the pH was raised, the number of negative charges per unit area on the diatomite surface was enhanced, consequently enhancing the electrostatic forces of attraction between the sorption sites and the metal cations due to their positive charge.

Flores-Cano et al (2013) analyzed the uptake of heavy metals by diatomite sample from Jalisco (Mexico). The study was based on the mechanism of adsorption and the influence of the operating variables. One of the important operating variables studied was the cation exchange pH. Flores-Cano et al analyzed the role of pH on Cadmium (II) uptake by a diatomite. According to the study, as the pH of the medium was raised from 4 to 7, the uptake of Cadmium (II) by diatomite was enhanced 9.74 times. The increase in adsorption capacity was linked to the charge on the sorbent surface when the pH was raised from 4 to 7.

Nenadovic et al (2015) carried out a study on the uptake of cesium from radioactive solutions using natural diatomite from Rudovci, Serbia. Diatomite was characterized and used in the sorption studies which evaluated the role of pH and initial concentration of cesium. To study the effect of pH, Nenadovic et al. (2015) investigated Cs adsorption on diatomite at values of pH from 2.07 to 10.71. It was discovered that, the acidic solutions (pH 2 - 4) had low Cs adsorption due to competitive adsorption of H^+ ions, whereas pH > 6 had a sharp increase in adsorption due to cesium hydroxide precipitation.

The effect of pH on the uptake of uranium (VI) on diatomite and magnesium silicate/diatomite sorbent (MSD) was studied by Lu et al (2016). The uptake of uranium (IV) on diatomite and MSD was enhanced as the pH was raised from 3.0 to 6.0, achieved a constant value for the pH range of 6.0 to 7.5 and decreased for pH>7.5. The enhancement in sorption for the pH range from 3.0 to 6.0 was associated with the electrostatic forces attraction between positively

charged uranium (VI) species and negatively charged surface of the adsorbent. The decline in the adsorption of uranium (VI) for the pH>7.0 was associated with electrostatic forces of repulsion between the negative surface of the adsorbent and negative uranium (VI) species such as $UO_2(CO_3)_2^{2-}$ and $UO_2(CO_3)_3^{4-}$ species.

Salman et al. (2016) examined the variation Pb (II) ion sorption with pH on diatomite sample. The highest adsorption efficiency of lead (II) ions was observed when the pH was 4 but significantly reduced beyond the pH of 4. Because of the role of hydrolysis and precipitation in the sorption of Pb (II), the sorption yield was found to decrease with increasing pH above 4.

Lu et al (2017) studied the uptake of uranium (VI) by the magnesium-silicate-diatomite. The raw and the treated diatomite were characterized, equilibrated with uranium (VI) and the effect of pH and ionic strength investigated. The results on the variation of pH indicated that the adsorption of uranium (VI) was enhanced when the pH was increased from 3.0 to 6.0, remained constant in the pH region of 6.0 to 7.5 and showed a decline for pH values greater than 7.5.

El Sayed (2018) conducted an investigation on the uptake of heavy metals by the Egyptian diatomite. The diatomite sample was characterized and its sorption properties studied under the influence if contact time, pH and diatomite content. Characterization involved determination of diatomite morphology by done by scanning electron microscope and identification of mineral phases by X-ray diffraction method. El Sayed (2018) investigated the influence of varying the pH between 2.0 and 8.0 on the adsorption of heavy materials by the diatomite from El-Fayoum, Egypt. As per the study results, the percentage of heavy metals removed was noted to increase as the pH increased and was maximized at pH of 4. An increase in pH was found to enhance the density of negative charge on the active sites of the adsorbent, thus enhancing electrostatic forces of attraction between heavy metals (M^{2+}) and the diatomite surface.

2.4.4 Variation of ions removal with contact time

Sheng et al (2008) investigated the uptake of thorium (iv) on the diatomite (Zhejiang province, China) under different operating conditions of temperature, pH, contact time and ionic strength. From the study on the effect of contact time on adsorption of Th (IV) by diatomite, the observed results showed that the uptake of thorium (IV) by diatomite was found to increase rapidly at the initial stage of contact, but as equilibrium was approached, the uptake of Thorium (V) remained constant with increase in contact time.

Caliskan et al (2011) carried out a study on the uptake of zinc (II) on diatomite and manganese-oxide modified diatomite from the Caldran region of Lake Basio Anatolia (Turkey). The diatomite was characterized and its kinetic and equilibrium adsorption properties investigated. The study examined the influence of contact time, pH, temperature and initial concentration on the adsorption properties of diatomite for zinc (II). On the effect of contact time on the uptake of zinc (II) ions by diatomite, Caliskan et al (2011) indicated that the sorption of Zn was fast at the start but slowed and achieved a constant value as contact time was increased.

Irani et al (2011) carried an investigation on the uptake of lead on Iranian clays namely; diatomite, dolomite and perlite. The effect of pH, contact time and the metallic concentration (at time $t = 0$) on the sorption properties of diatomite, dolomite and perlite for lead were studied. On the role of contact time on the adsorption properties of diatomite, the results indicated that the lead ions concentration in the aqueous phase was greater than 80 percent of their equilibrium concentration after a duration of 1 hour while the equilibrium was achieved after 2 hours

Yusani et al (2012) conducted an investigation on the uptake of thorium (IV) on diatomite samples from Turkey which were first either treated by calcination or by flux-calcination. The diatomite sample was characterized and its adsorption properties determined at different operating levels of initial metallic concentration, pH, temperature and contact time. The variation of the uptake of Th (IV) on diatomite with contact time was evaluated by contacting Th (IV) with 50 mg\L initial concentration with "calcined diatomite (C-D) and flux calcined diatomite (FC-D)" for 10 to 90 minutes at pH 4.0 for both adsorbents. According to the study, there was a minor increase in the adsorption yield as the contact shaking time was increased and an equilibrium was arrived "at 98% and 89% sorption within 20 min" for calcined and flux-calcined diatomite, respectively.

Ibrahim et al (2013) studied the variation of the uptake of Cd (II), Cu (II), Pb (II), Ni (II), and Zn (II) by the Egyptian diatomite with contact time. The study indicated that the percentage of the target cations removed was raised as the time allowed for adsorption was increased until equilibrium was reached, at which point the removal percentage remained constant.

Salman et al (2016) studied the effect of time of adsorption on the uptake of Pb (II) ions on diatomite sample from Turkey. The rate of sorption of Pb (II) was initially higher as the number of free active sites and the concentration of Pb (II) were high. The optimal contact time for Pb

(II) was observed to be 75 minutes, after which the removal rate of Pb (II) was observed to gradually decrease as contact time increased.

ElSayed (2018) investigated the influence of adsorption time on heavy metal sorption on a diatomite sample from El-Fayoum, Egypt. The removal percentage began rapidly and then slowed, which was explained by the large surface area of diatomite at the start and the subsequent reduction in sorption sites with heavy metal uptake.

2.5 Synthesis, implication and identified knowledge gaps

From the work done on the application of diatomite for sorption of contaminants from liquid waste, it is evident that not much has been done on the influence of particle size on the sorption properties of diatomite. Most studies have failed to explain how the mineral phase composition of diatomite affects its sorption properties. While chemical compositions of diatomite from various studies indicate comparable constituents, their cation exchange capacities have shown great variation. Different methods have been employed by various authors in determination of cation exchange capacity. It is not clear what proportion of the variation in the cation exchange capacity may be explained by the variation in the method used.

In general, most of the published studies investigated the capacity of their respective adsorbent materials in either single or bi-solute competitive sorption of radionuclides from liquid solutions. However, in practice, most radioactive wastes are composed of several radionuclides in different concentrations, therefore, a study of the efficiency of various adsorbents for sorption of the target radionuclides from multicomponent solution is more practically relevant (Rahman et al, 2011).

It has been observed that, generally, Cobalt, Strontium, and Uranium in their metastable state have high environmental impact. In most studies, the Cesium, Cobalt, Strontium, and Uranium sorption used were either, from actual or prepared liquid radioactive waste streams. However, studies of sorption of Zn from liquid solutions are limited (Rahman et al, 2011).

Sorption is among the most well-established method for management of hazardous radionuclides from liquid waste streams. The big merit of adsorption is the potential for removing very small quantities of contaminants from large volumes of liquid wastes (Aytas et al 1999). In addition, the adsorption method is robust. The robustness of sorption or ion exchange is dependent on the variety of sorbent materials that have been tested for the capture of radionuclides from waste streams. However, most natural sorbents have limited properties

such as; poor stability under radiation field and low removal capacities at high temperature, whereas synthetic sorbents are expensive.

Some of the notable characteristics of diatomite include; high permeability, high porosity, small particle size, high surface area, chemical inertness and low thermal conductivity (Bailey et al, 1999). Diatomite being an inorganic sorbent is of great importance due to its selectivity towards certain metal ions, outstanding stability against radiation, chemical attack and compatibility with potential immobilization materials (Ibrahim, 2010).

Various studies that have been conducted on the capacity of diatomite for the uptake of toxic metal ions show that, natural or modified diatomite is a promising sorbent due to its affordability and high efficiency. The studies reveal that diatomite exhibits superiority over other sorbents such as synthetic resin, activated carbon, carbon nanotubes, mesoporous silica, clay minerals, natural and synthetic zeolite and biomass (Nenadović1 et al, 2009). Table 1.1 compares the capacity of various sorbent materials for adsorption of cobalt from water.

Table 2.2: The adsorption capacities of various adsorbents for cobalt uptake from water, Sheng et al (2012)

Sorbent	$q_{\max}\left(\frac{mol}{g}\right)$
Nedalco anaerobic granular sludges	2.06×10^{-4}
Eerbeek anaerobic granular sludges	1.95×10^{-4}
Bone char	1.81×10^{-4}
Rhytidiadelphus squarrosus (moss)	1.23×10^{-5}
Lemon peel as biosorbent	3.67×10^{-4}
Almond green hull	7.58×10^{-4}
Granular activated carbon	1.98×10^{-5}
Magnetic multiwalled carbonnanotube/iron oxide composites	1.50×10^{-4}
Kaolinite	2.45×10^{-5}
Al-pillared bentonite	6.44×10^{-4}
Palygorskite	1.48×10^{-4}

Methacrylic acid/acrylamide monomermixture grafted poly(ethyleneterephthalate) fiber	4.53×10^{-4}
Sepiolite	0.79×10^{-4}
Diatomite	6.91×10^{-4}

Diatomite is mined locally in Kenya and is abundantly available. However, its characterization and usage in the management of radioactive wastes have not been extensively studied. It was on this basis, that this study was aimed at establishing whether diatomite sorbent has the potential of use as sorbent material for radionuclides following its use in the treatment of heavy metal contaminated waste water streams.

CHAPTER 3: MATERIALS AND METHODS

3.1 Introduction

In this chapter, the materials and methods used in the evaluation of the local diatomite samples from Kariandusi Mining Area, Kenya are presented and discussed. In general, the chapter is presented as follows; the materials and methods used to determine the chemical composition, mineral phase composition, natural radioactivity, particle size distribution and cation exchange capacity of diatomite are presented in section 3.2 - 3.5. Section 3.6 describes the materials and methods used to determine the sorption capacity of diatomite as well as the Influence of diatomite content, initial cation concentration, contact time and pH on sorption.

3.2 Chemical composition of Diatomite

Figure 3.1 shows the portable S1 Titan 600 series Bruker x-ray Fluorescence unit used in the determination of the elemental content in diatomite samples. Prior to sample analysis, three samples were prepared in pellet forms weighing between 5 - 10 gm from homogeneously pulverized ground samples of diatomite. The facility is available for use at the Department of Mines and Geology, in the Ministry of Energy.

The samples were irradiated for 60 seconds and the spectrum of the elemental profile was analyzed for content using software called Bruker Remote ctrl.

Figure 3.1: S1 Titan Brunker Model S1 Titan 600 series 600N 3187- MFG May 29, 2015, Mines and Geology Department, MOE, Kenya

3.3 Determination of mineral phase composition of diatomite

The crystalline phases of diatomite were identified using an X-ray diffractometer at the Department of Mines and Geology, MOE. Figure 3.2 depicts the Bruker XRD spectrometer used in this study.

Figure 3.2: Brunker D2 2 Gen Phaser Machine -Model D2 Phaser SSD 160 A 26-X1-A2DOB2B1, Mines and Geology, MoE , Kenya

In order to identify the phases, a powdered sample of diatomite was loaded into the sample holder and then the sample gently pressed into cavity and smoothed over. The sample was then loaded onto the stage and locked in place. Figure 3.3 shows the sample loading mechanism of sample holders for irradiation in the spectrometer chamber.

Figure 3.3: Diatomite samples for Brunker D2 Phaser analysis, Mines and Geology, MoE Kenya

The diffraction angle "2 theta" was set to be between 7º to 80º range which was specifically chosen to contain the diffraction positions for polymorphs of silica. The sample was flagged to position and subjected to x-ray beam irradiation for 6 minutes. The spectrum was obtained and the crystalline species identified by comparing the species present with the mineralogical databases using Bruker "DIFFRAC.SUITE EVA" software package (Giencke, 2007).

3.4 Radioactivity characterization of Diatomite Samples

The diatomite sample was radiologically analyzed using "a p-type intrinsic hyper pure germanium (HpGe) coaxial detector" vertically "mounted and coupled to a 3 kV digital high voltage source" available at the University of Nairobi's Institute of Nuclear Science and Technology. "Calibration sources containing ^{133}Ba, ^{22}Na, ^{137}Cs, ^{54}Mn and ^{60}Co" were used to calibrate the HpGe detector for energy and relative efficiency. For checking the efficiency of

the system's calibration, a performance test was done using IAEA standard reference materials "Soil-375, RGU, RGTh, and RGK" (Otwoma et al, 2012).

3.3.1 Sample Preparation and For Gamma Spectroscopy Analysis

The samples were crushed to a size of about 2 mm and oven dried for about 24 hours at 110 C in order that the weight achieved remains constant. The diatomite samples were then dried in air before being pulverized and homogenized to a size of approximately 100 μm. Approximately 300g of diatomite sample was weighed into a plastic container which was tightened and properly sealed with aluminium foil to stop ^{220}Rn and ^{222}Rn from escaping. The sealed sample was then stored for 30 days to achieve "secular equilibrium between thorium and radium and their decay products" (Otwoma et al, 2012).

Gamma-ray spectral analysis was performed on a diatomite sample to determine the activity concentrations of ^{238}U, ^{232}Th, and ^{40}K. To calculate the activity concentrations of ^{238}U and ^{232}Th, it was assumed that they had reached a secular equilibrium with their decay products, and thus the gamma-ray spectrum peaks found in the sample were attributed to ^{40}K and decay products of^{238}U and ^{232}Th.

The concentrations of the ^{238}U series were determined using counts at gamma transition energies of 351.9 keV due to ^{214}Pb and 609.2 keV due to ^{214}Bi. Similarly, the gamma transition energies of 238.6 keV for ^{212}Pb, 583.1 keV for ^{208}Tl, and 911 keV for ^{228}Ac were used to calculate ^{232}Th concentrations. The activity of ^{40}K was calculated based on its 1460 keV gamma-line.

Since the distribution of ^{238}U,^{232}Th and ^{40}K is not the same in diatomite, a single value describing the gamma output from the three radionuclides was calculated using equation 3.1 below.

$$\mathrm{Ra_{eq}} = A_U + 1.43A_{\mathrm{TH}} + 0.077\mathrm{A_K} \qquad (3.1)$$

where $A_U, A_{TH}$and A_K are the activity concentrations of $^{238}_{92}U, ^{232}_{90}Th$ and $^{40}_{19}K$ respectively (Isinkaye & Ajayi, 2006).

3.5 Particle size analysis and measurements of diatomite

Figure 3.4 show the particle size analysis and measurements done using the ROTAP screen shaker, weighing balance and Sieves of different aperture sizes.

Prior to the particle size determinations, the sieves and receiving pan were cleaned and weighed. The diatomite sample was then weighed. The sieves were then arranged in order, from largest opening sieve located at the top to smallest opening sieve at the bottom. The diatomite sample was loaded on the top sieve and the complete sieve stack fitted on the sieve shaker. The shaker was switched on for 15 minutes.

Figure 3.4: Rotap screen shaker for particle size measurements, Mines and Geology, MoE

The weight of each sieve and receiving pan were recorded so as to determine the weight of diatomite particles retained on each screen and the receiving pan.

3.6 Determination of Cation Exchange Capacity of diatomite

Determination of diatomite's cation exchange capacity was carried out using the SW-846 Test Method 9081 (EPA, 2020). The diatomite samples were first mixed with sodium acetate solution to allow the added sodium cations to exchange with the matrix cations. To remove the excess sodium acetate solution, the sample mixture was washed with isopropyl alcohol. To exchange the adsorbed sodium for ammonium, an ammonium acetate solution was added. The concentration of sodium displaced from the matrix was then determined using a flame photometer technique.

3.6.1 The reagents used in determination of CEC of diatomite

1.0 N sodium acetate, 1.0 N ammonium acetate, and 99 percent isopropyl alcohol were used as reagents. To make I.0 N of sodium acetate, 136 g of $NaC_2H_2O_2 \cdot 3H_2O$ was dissolved in distilled water and diluted to 1,000 mL. By adding a few drops of acetic acid and NaOH solution, the pH of this solution was raised to 8.2.

To make 1.0 N of ammonium acetate, 114 mL of glacial acetic acid (99.5 percent) was diluted with water to a volume of 1 liter. The solution was then treated with 138 mL of concentrated ammonium hydroxide (NH_4OH). Distilled water was then added to make a volume of approximately 1,980 mL.

The pH of the resulting solution was determined, and NH_4OH was added to achieve a pH of 7. The solution was diluted to a volume of 2 liters with distilled water.

3.6.2 Sodium acetate method of determining CEC of diatomite

4 g of medium textured (>50% of the particles diameter ≥0.425 mm) diatomite was put into a 50-mL centrifuge tube.

33 mL of 1.0 N NaOAc solution was added to the centrifuge tube, the tube was then stoppered, mechanically shaken for 5 min, centrifuged until clear supernatant liquid was obtained and the liquid decanted. This was repeated three more times until all the cations in the diatomite matrix are exchanged with sodium cations.

Figure 3.5 shows the diatomite samples in centrifuge tubes placed on the Edmund Buhler mechanical shaker. Figure 3.6 shows the diatomite sample placed in the MSE centrifuge.

Figure 3.5: Edmund Buhler 7400 Tubingen mechanical shaker, at KEFRI, Kenya

Figure 3.6: Diatomite samples on MSE Centrifuge, KEFRI

33 mL of isopropyl alcohol (99%) was added, the tube stoppered, mechanically shaken for 5 min, and centrifuged until a clear supernatant liquid was obtained and the liquid decanted. This step was repeated twice.

33 mL of NH_4OAc solution was then added, the tube stoppered, mechanically shaken for 5 min, and centrifuged until clear supernatant liquid was obtained and the washing decanted into a 100-mL volumetric flask. This step was repeated twice. The mixture was diluted to the 100-

mL mark with NH_4OAc and the concentration of sodium determined by Corning 400 flame photometer method. Figure 3.7 shows the Flame Photometer used in this study.

Figure 3.7: Corning 400 Flame Photometer, Kenya Bureau of Standards, Kenya

The method for the flame photometric determination of the concentration of sodium displaced from the diatomite matrix is described in section 3.6.3.

Once the concentration of sodium displaced from the diatomite matrix was found, the CEC was calculated using equation 3.2:

$$\mathrm{CEC} = \frac{[\mathrm{Na}^+] \times \mathrm{V} \times 100}{\mathrm{m} \times \mathrm{EW}_{\mathrm{Na}}} \qquad (3.2)$$

where CEC denotes the cation-exchange capacity per 100 g of diatomite in meq/100 g; $[Na^+]$ is the sodium concentration in mg/l; V denotes the volume of the solution in litres; m is the mass of diatomite in g and EW_{Na} is the equivalent weight of sodium in mg/meq. Substituting for $V = 0.1\ l, m = 4\ g, EW_{Na} = 22.99\ mg/meq$ yields equation 3.3 below in which the concentration of $[Na^+]$ obtained from the CEC trials substituted to obtain CEC values.

$$\mathrm{CEC} = \frac{[\mathrm{Na}^+]\frac{mg}{l} \times 0.1\ l \times 100\ g}{4\ \mathrm{g} \times 22.99\frac{\mathrm{mg}}{\mathrm{meq}}} \qquad (3.3)$$

3.6.3 Flame Photometric Determination of the Concentration of Sodium Displaced from the Diatomite Matrix

For the analyses of concentration of sodium using flame photometric analysis, standards of 2, 4, 6, 8 and 10 ppm were prepared. Prior to analyses, the standards were run and the intensity signal was plotted against the concentration for purposes of calibrations. A spiked sample of 7.5 ppm sodium was prepared to gauge the stability of the system. The standards of 2, 4, 6, 8 and 10 ppm were run in the Corning 400 flame photometer to obtain intensity values. A scatter plot of the concentrations of standards against the intensity meter readings was constructed and a line of best fit drawn. The samples were diluted by a factor of 10 and were run and the corresponding intensity readings values determined from which the concentration of sodium in the samples were determined after corrections for dilution.

3.7 Determination of sorption capacity of Diatomite

Sorption of a reactive radionuclide involves four steps. The first step is the physical attachment, followed by bulk fluid transport, film transport and lastly diffusion into the pores of the sorbent. The rate-limiting steps controlling the sorption process are film transport and pore diffusion. At equilibrium, there is a distinct distribution of ions between the liquid phase and the solid sorbent phases. Consequently, sorption experiment involves equilibrating a specified mass of sorbent at specific temperature and pressure with known volume of specific concentration. The quantity ions removed from the solution by sorption on the sorbent is determined from the difference between the initial concentration of ions the solution and the equilibrium concentration ions solution (Saint-Fort, 2018) .

The sorption capacity of diatomite was studied by equilibrating it with prepared aqueous solutions containing ions of Ba, Zn and Co. The effects of adsorbent content, contact time, pH and initial cation concentrations on sorption capacity were investigated.

For the sorption capacity studies, the initial and final concentrations of metals in the solutions were determined by Total X-ray Fluorescence (TXRF) facility available at the Institute of Nuclear Science and Technology, Nairobi.

3.7.1 Preparations of Simulated Radioactive liquid Waste Used in This Study

The behavior of radionuclides can be correlated to stable elements in the same chemical group with respect to their sorption. Consequently, sorption mechanisms can be readily deduced accordingly. The mechanisms of sorption of radionuclides show that the sorption process is dependent on the attraction force between the individual molecules, atoms or ions of a sorbate and the sorbent surface (Saint-Fort, 2018). The sorption of radionuclides can be deduced by studying their stable forms as done by Sheng et al (2008), Yusan et al (2012) and Nenadovic et al (2015).

This study targeted removal of Co, Zn and Ba in their stable forms for possible application in the removal of ^{60}Co, ^{133}Ba and ^{65}Zn which are some of the radionuclides typically present in liquid radioactive wastes (IAEA, 2003).

The simulated radioactive liquid waste, was prepared from analytical grade solutions of Ba $(NO_3)_2$, Co $(NO_3)_2$ and Zn $(NO_3)_2$ compounds with each cation concentration varying from 0.5 mg/l to 10.7 mg/l.

3.7.2 Variation of removal of ions with adsorbent content

The variation of removal of ions with adsorbent content was studied by varying the quantity of diatomite in the simulated radioactive liquid waste while maintaining pH, contact time and the initial concentrations of Ba, Co and Zn constant.

Different masses; 0.5 g, 1.0 g, 1.5 g, 2.0 g, 2.5 g, 3.0 g of diatomite were contacted with 100 ml of simulated liquid wastes (0.5 mg/L) in 250 ml sample bottles and mixed for 4 hours at room temperature with constant shaking at 175 rpm on Edmund Buhler 7400 Tubingen mechanical shaker.

After 4 hours, the contents of the flasks were filtered. Residual concentrations of Ba, Co and Zn in the filtrate were determined using Total X-ray Fluorescence (TXRF).

The removal efficiency(η_R) was calculated using the equation 3.4:

$$\% \, \eta_R = \left[\frac{C_i - C_t}{C_i}\right] . 100 \qquad (3.4)$$

where C_i is the initial concentration of cation (mg L^{-1}) and C_t is the final concentration of the cation (mg L^{-1}) at a time t.

The quantity of metals adsorbed $q_m \left(\frac{mg}{g}\right)$ was determined by equation 3.5:

$$q_m = \frac{(C_i - C_t) * V}{m} \qquad (3.5)$$

Where C_i is the initial concentration of cation (mg L^{-1}), Ct is the final concentration of the cation (mg L^{-1}) at a time t, V: is the volume of solution (L), m: the mass of the diatomite in grams.

The moles of metals adsorbed at a given time $q_t \left(\frac{mol}{g}\right)$ were estimated by equation 3.6:

$$q_t = \frac{(C_i - C_t) * V}{1000 \times mW} \qquad (3.6)$$

Where C_i is the cation concentration at a time $t = 0$ in (mg L^{-1}), Ct is the final concentration of the cation (mg L^{-1}) after a time span of t, V represents the volume in (L) of the simulated waste contacted with the diatomite, m stands for the diatomite mass in grams and W is the molecular of the metal (g/mol).

3.7.3 Variation of removal of ions with initial metallic concentration

In order to determine the effect concentration of Co, Zn and Ba, 1 L of simulated liquid waste solution containing 7.458 mg/L of Co, 8.289 mg/L of Zn and 10.662 mg/L of Ba were prepared. The pH of the prepared solution was adjusted to 6 by addition of drops 0.1M HNO_3 and 0.1M NaOH solutions accordingly and was measured by HORIBA LAQUA PH/ION METER F72 available at Kenya Forestry Research Institute (KEFRI), Kenya.

In the initial set of runs, 100 ml of the prepared simulated waste solution was measured into three separate 250 mL sample bottles. The simulated waste solutions in the three sample bottles were treated with diatomite contents of 2.0 g, 2.5 g and 3.0 g of diatomite respectively. The

samples were sealed, capped and subjected to constant shaking at 175 rpm on Edmund Buhler 7400 Tubingen mechanical shaker for 4 hours. The contents of the sample bottles were then filtered through the Whatman 542 qualitative filter paper, diameter 125 mm.

The initial concentrations of Co, Zn and Ba in the prepared simulated waste solution and the final concentrations in the filtrate, were determined using Total X-ray Fluorescence (TXRF) spectrometer at the Institute of Nuclear Science, University of Nairobi. The removal efficiency (η_R) was calculated using equation 3.4.

Four other sets of runs were prepared except that the concentrations of Co, Zn and Ba were halved for each successive set by diluting with simulated waste solution with double distilled water for analysis.

3.7.4 Variation of removal of ions with the pH

To study the variation of the removal of ions of diatomite with pH, the pH of the simulated waste solution was varied between 2 and 10, while the content of diatomite, the contact time and the initial concentrations of Co, Zn and Ba were kept constant.

1 L of simulated waste solution containing 5.999 mg/L of Co, 5.982 mg/L of Zn and 6.877 mg/L of Ba was prepared. 100 ml of the prepared simulated solution was measured into each of the five 250 ml sample bottles and the pH of the simulated waste solutions in the five sample bottles adjusted to 2, 4, 6, 8 and 10, respectively by addition of drops 0.1M HNO_3 and 0.1M NaOH solutions accordingly and measured by HORIBA LAQUA PH/ION METER F72, available at Kenya Forestry Research Institute (KEFRI), Kenya.

The 100 ml of simulated waste in each of the five sample bottles was treated with a content of 2.5 g of diatomite. The five sample bottles were tightly capped and sealed and were then subjected to constant shaking at 175 rpm on Edmund Buhler 7400 Tubingen mechanical shaker for 4 hours.

The contents of the sample bottles were filtered through the Whatman 542 qualitative filter paper, diameter 125 mm. The initial concentrations of Co, Zn and Ba, in the prepared simulated waste solution and the final concentrations, in the filtrate were determined using Total X-ray Fluorescence (TXRF) spectrometer at the Institute of Nuclear Science & Technology, University of Nairobi, Kenya. The removal efficiency (η_R) was calculated using equation 3.4.

3.7.5 Variation of removal of ions with contact time

To investigate the variation of removal of ions with the contact time, 1 L of simulated waste solution containing 7.458 mg/L of Co, 8.289 mg/L of Zn and 10.662 mg/L of Ba was prepared.

The pH of the prepared simulated waste solution was adjusted to 6 by addition of drops 0.1M HNO_3 and 0.1M NaOH solutions accordingly. 100 ml of the prepared was measured into each of the six 250 ml sample bottles. For each sample bottle was added with 2.5 g of diatomite. The sample bottles were tightly sealed and capped. The six samples were then subjected to constant shaking at 175 rpm on Edmund Buhler 7400 Tubingen mechanical shaker for 1 hour, 2 hours, 3 hours, 4 hours, 5 hours and 6 hours, respectively.

At the end of each shaking period, the corresponding sample bottle contents was filtered through the Whatman 542 qualitative filter paper, diameter 125 mm. The initial concentrations of Co, Zn and Ba (in the prepared simulated waste solution) and the final concentrations (in the filtrate) were determined using Total X-ray Fluorescence (TXRF) spectrometer at the Institute of Nuclear Science, University of Nairobi from which the removal efficiency (η_R) was calculated.

3.7.6 TXRF method used for determination of concentrations of Co, Zn and Ba

All concentration measurements of Co, Zn and Ba were performed using the benchtop TXRF spectrometer S2 PICOFOX, available at the Institute of Nuclear Science, University of Nairobi, Kenya. Figure 3.8 shows the TXRF spectrometer at the Institute of Nuclear Science &Technology, University of Nairobi.

3.7.6.1 Procedures used for Cleaning of Sample Carriers Prior To TXRF Analysis

Prior to the analyses with the TXRF method for determination of concentrations of Co, Zn and Ba, all the sample carriers used were thoroughly cleaned according to the procedure provided by the laboratory protocols for sample preparation and analysis with TXRF.

The sample carriers were first subjected to mechanical pre-cleaning with a fluff-free cleaning tissue. The pre-cleaned sample carriers were then mounted on the washing cassette, transferred to a glass beaker filled with 5% RBS cleaning solution to the level enough to cover the sample carriers and heated for 5 minutes on a heating plate. The sample carriers were then thoroughly rinsed with double distilled water. The washing cassette with the sample carriers were then transferred into a glass beaker filled with 10% nitric acid and heated for two hours on a heating

plate, placed in a chemical fume hood. The sample carriers were then transferred into a beaker filled with distilled water and heated on a heating plate for five minutes. The sample carriers were then rinsed with double distilled water. The clean sample carriers were then dried on a hot plate and allowed to cool to room temperature.

The cleaned and dry sample carriers were scanned for any residual contaminations and those whose spectrums were free from impurities, were identified and selected for use. The selected sample carriers were spotted with 10 μl of silicon solution, dried over a hot plate and allowed to cool to room temperature and scanned for contaminations and eventual sample preparation.

Figure 3.8: BRUKER S2 PICOFOX TXRF available at Institute of Nuclear Science & Technology

3.7.6.2 Sample preparation and analysis with TXRF

In order to prepare the sample for TXRF analysis, 5 ml of the sample was measured and mixed with 10 μL to 50 μL of 1000 ppm Yttrium internal standard such that the concentration of

Yttrium in the matrix was close to the range of the expected concentrations of 0.5 mg/l to 10 mg/l of Co, Zn and Ba ions in the sample. $10\ \mu L$ of the prepared sample was then spotted at the centre of each sample carrier of a triplicate set of sample carriers.

The triplicate of sample carriers was then dried on the hot plate and allowed to cool to room temperature. The dry samples on the carriers were then analyzed with TXRF machine for element content following irradiation for specific times. The results of the triplicate for each sample were then averaged for each sample analyzed.

CHAPTER 4: RESULTS AND DISCUSSION

4.1 Introduction

In this chapter, the results and discussion of the evaluation of the local diatomite from Kariandusi Mining Area, Kenya are presented. In general, the chapter is arranged as follows; such that the chemical composition, natural radioactivity, mineral phase composition, particle size distribution and cation exchange capacity of diatomite are presented in Section 4.2 to Section 4.6. The results of the sorption capacity of diatomite as well as the Influence of diatomite content, initial cation concentration, contact time and pH are covered in Section 4.7.

4.2 Chemical composition of the diatomite samples

The results of the chemical composition of diatomite of are presented in Table 4.1, while Figure 4.1 shows the bar chart variations concentrations of the chemical components present in diatomite samples.

Table 4.1: Table of chemical composition of diatomite samples

Element/ Oxide Name	Test 1 Concentration (%)	Test 2 Concentration (%)	Test 3 Concentration (%)	Aver (%)	Standard deviation
MgO	0.000	0.000	2.895	0.965	1.671
Al_2O_3	2.087	1.353	2.274	1.905	0.487
SiO_2	92.583	94.049	88.291	91.641	2.992
P_2O_5	0.033	0.073	0.077	0.061	0.024
K_2O	0.704	0.609	0.836	0.716	0.114
CaO	2.602	2.115	3.279	2.665	0.585
Ti	0.192	0.121	0.131	0.148	0.038
Fe	1.563	1.369	1.898	1.610	0.268
Other	0.236	0.311	0.319	0.289	0.046
Total	100	100	100	100	

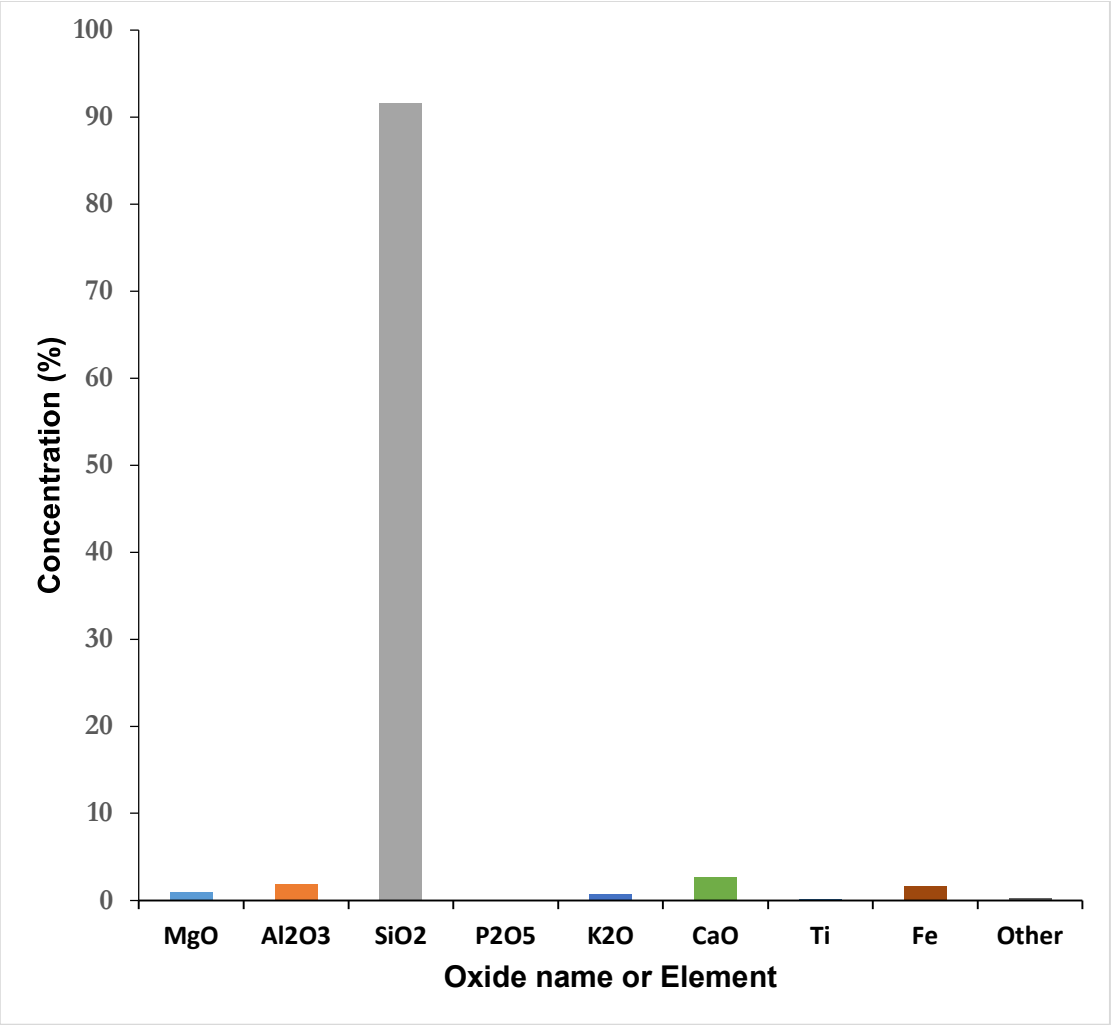

Figure 4.1: Chemical composition of diatomite from Kariandusi Mining Area, Kenya

According to figure 4.1, the principal component of the diatomite sample was silica (SiO_2), which accounted for 91.64 percent of its weight. Other oxides found in diatomite Al_2O_3, CaO, MgO, K_2O and P_2O_5, with weight percentages of 1.91, 2.67, 0.97, 0.72, and 0.06, respectively. The concentrations of the target metals of interest, Zn, Co, and Ba, were found to be negligible in diatomite. The high silica content of diatomite is characteristic of clay minerals that make good adsorbents, a finding that is consistent with related previous research, Koyuncu (2012).

4.3 The mineral phase composition of diatomite

Figure 4.2 shows the XRD spectrum of mineral constituents of diatomite samples. In general, the diatomite sample was characterized by one major peak at 22.1° and a minor peak at 36.3°.

The peak at 22.1° corresponded to the cristobalite, a polymorph of silica, while the peak at 36.3º was due to presence of ringwoodite. Cristobalite is the dominant phase with its peak approximately three times taller than that of ringwoodite.

The typical natural diatomite rock is primarily made of amorphous silica. Calcination converts amorphous silica to crystalline polymorph known as cristobalite. Ringwoodite is a secondary silicate formed during the calcination process at a temperature of 1000ºC. (Nattrass et al., 2015).

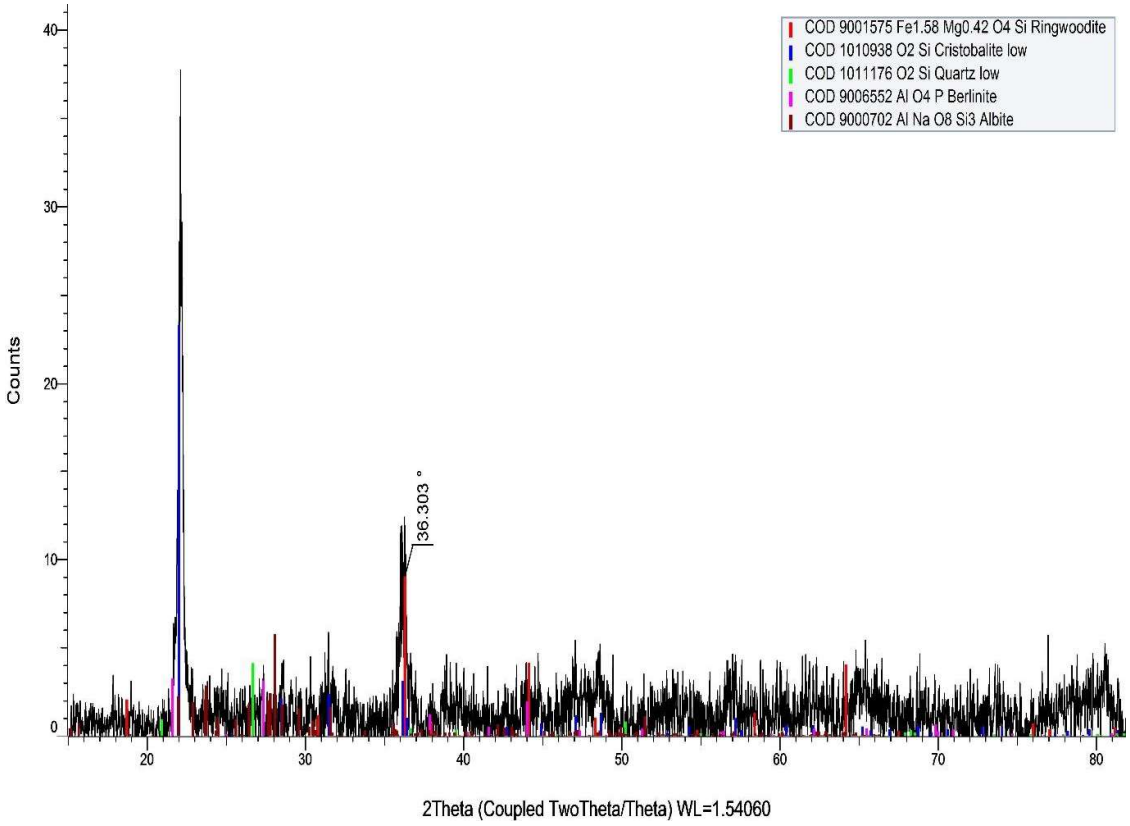

Figure 4.2: XRD pattern of diatomite sample from Kariandusi mining area, Kenya

4.4 Radioactivity characterization of diatomite samples

Natural radioactivity is one of the important physical properties of diatomite. Naturally occurring radioactive isotopes in the diatomite come from ^{238}U,^{232}Th, and ^{40}K in the parent mineral rock.

Table 4.2 gives a summary of the specific activities of ^{232}Th, ^{238}U and ^{40}K obtained for diatomite samples analyzed by gamma spectrometry. The radium equivalent activity of diatomite was found to be 78.00 ± 13.46 Bq/Kg which was lower the stipulated safe limit of 370 Bq/Kg (Isinkaye & Ajayi, 2006).

Table 4.2: Activity concentration of 238U, 232Th, and 40K in diatomite samples from Kariandusi mining area, Kenya

Radionuclide	Line energy (Kev)	Specific activity (Bq/Kg)
TH-232	238.36	12.89 ± 4.1
U-238	351.55	41.42 ± 6.9
K-40	1460.80	235.66 ± 9

4.5 The particle size distribution of the diatomite samples

In order to determine the particle size distribution for diatomite, a weighed sample of diatomite was loaded on the top of a set of sieves with decreasing aperture sizes and mechanically shaken using a Rotap screen shaker. The weight of diatomite particles retained on each screen was determined. The sample weight of diatomite used was initially 347 g.

Tables 4.3 shows the results for the study on particle size distribution of diatomite sample. Figure 4.3 shows the corresponding plot for particle size distribution. The particle size distribution curve in figure 4.3 indicates that 10% of the particles (d_{10}) have diameter less than 171 µm, 50% of particles (d_{50}) have a diameter less than 589 µm, while 90% of particles (d_{90}) are less than 1523 µm.

The adsorption of target metals from solutions is characterized by the mass transfer of the target metals on to the surface of the sorbent followed by subsequent diffusion into the interior of the sorbent. The rate of adsorption is governed by the limiting step. When the particle size of the adsorbent is reduced, the diffusion path length inside the sorbent is reduced and this reduces the diffusion limitation. Hence adsorption capacities will be higher smaller particle sized sorbents especially in the nanometer range. While the use of sorbents with particle size in the nanometer range will realize higher adsorption capacities, the difficulty of regeneration of the adsorption column due to large pressure drops is a critical factor to be considered in selection of the optimum particle size. It is worth noting that for porous adsorbents like diatomite, grinding does not bring about significant change in the surface area as the principal surface area comes from the pores (usually in the nanometer range) which are much smaller than the particle size.

Table 4.3: Particle size distribution of diatomite from Kariandusi Mining area, Kenya

Particle Diameter (μm)	Mass (g)	Percentage	Cumulative percentage	Percentage finer
$D > 2000$	8	2	2	98
$1000\ \mu m < D < 2000\ \mu m$	56	16	18	82
$710\ \mu m < D < 1000\ \mu m$	76	22	40	60
$425\ \mu m < D < 710\ \mu m$	79	23	63	37
$150\ \mu m < D < 425\ \mu m$	101	29	92	8
$75\ \mu m < D < 150\ \mu m$	21	6	98	2
$D < 75\ \mu m$	6	2	100	0
Total	**347**	**100**		

Generally, smaller particles offer larger surface areas for sorption than larger particles. However, smaller particle sizes are costlier to process and cause flow blocking problems in an adsorbent bed. Hence the optimum particle size for sorption of Co, Zn and Ba can only be obtained by conducting a further investigation of the role of diatomite particle size on the sorption capacity for Co, Zn and Ba.

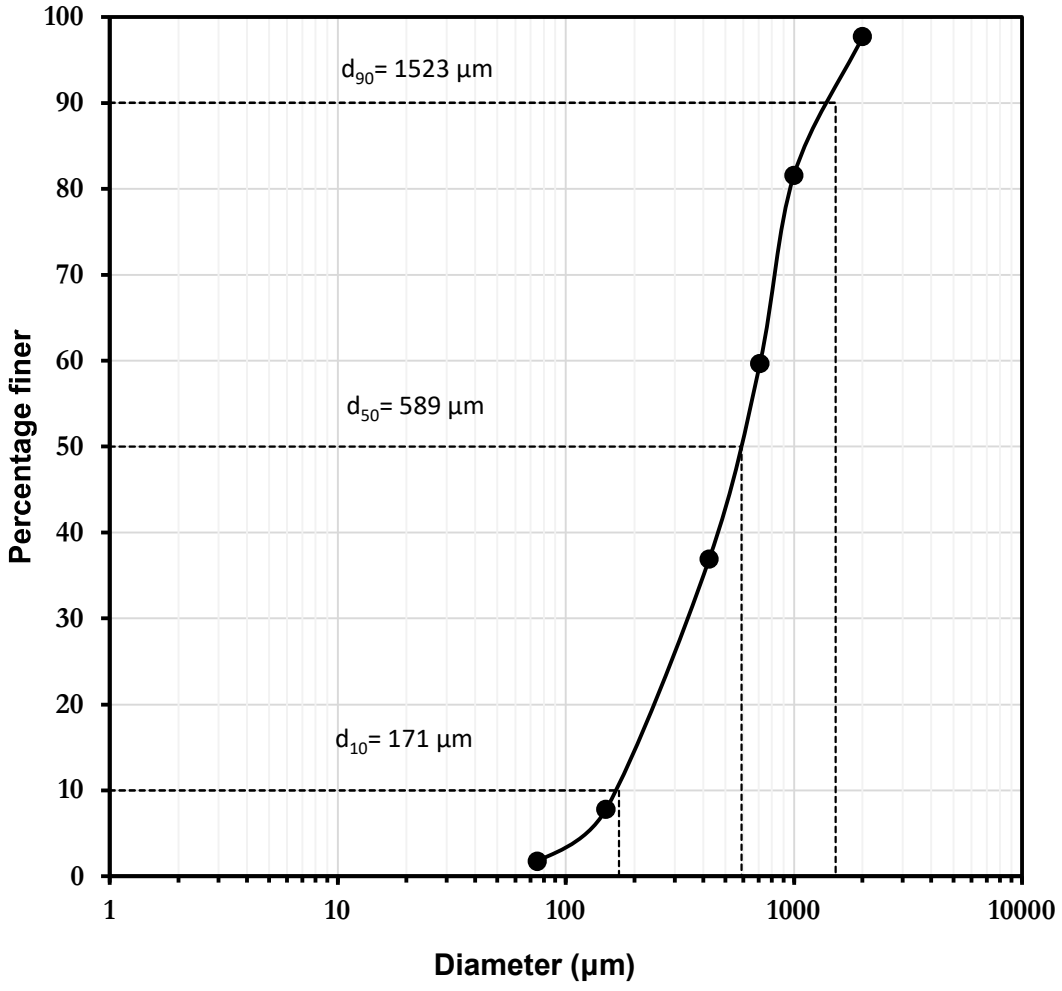

Figure 4.3: Particle size distribution of diatomite from Kariandusi Mining area, Kenya

4.6 Cation exchange capacity (CEC) of the diatomite samples

The SW-846 test method 9081 (EPA, 2020) was used to determine the CEC of diatomite. To exchange sodium cations with cations in the diatomite matrix, the sample of diatomite was

washed with excess sodium acetate. The unreacted sodium acetate was removed by reaction with isopropyl alcohol. So as to determine the amount of sodium cations in the diatomite matrix, the diatomite sample was mixed with ammonium acetate. The sodium cations in the diatomite matrix were replaced with ammonium ions while the ammonium ions in the solution were replaced with sodium cations. A flame photometer method was then used to determine the concentration of sodium displaced from the matrix.

Prior to the measurements, the flame photometer was calibrated against standard sodium solutions in various concentration levels to determine the linear equation relating meter reading values with the concentration of sodium in the samples.

Table 4.4 and Figure 4.4 shows the results of the calibrations used in the determinations of sodium in the samples. In general, the calibrations correlation value of r^2 was 0.9979. The spiked sample of sodium gave a concentration of 7.7 ppm against the expected value of 7.5 ppm.

The linear equation relating intensity signal values (x) with the concentration of sodium in the standard (y) was found to be:

$$\boldsymbol{y = 0.1973x - 0.1304} \qquad (\mathbf{4.1})$$

Table 4.4: Intensity values for the calibration of flame photometer for determination of Na+ in samples

Standard [Na^+] in ppm	Meter reading
0	0
2	11
4	21
6	32
8	42
10	50

In Table 4.5, $\bar{x}$ and σ are the average and standard deviation of the cation exchange capacity (CEC) values of the four trials respectively. The CEC in meq/100g is a measure of the number

of negative charges per 100 g of the sorbent that can adsorb exchangeable cations. The CEC value for diatomite sample from Kariandusi, Kenya was 7.94 meq/100g (6.97 – 8.91) meq/100g, compared to 1.27 meq/g obtained by Flores-Cano et al (2013), 9.8 meq/100g and 11.3 meq/100g values obtained by (Belousov et al, 2019), 50 meq/100g obtained by Nenadovic et al (2015) and 80 cmol/kg obtained by Piri et al (2020). The difference between the CEC value obtained in this study and the values by other studies is due to the variation in the pH of diatomite, level and method of purification and the nature and quantity of natural clay minerals present in diatomite.

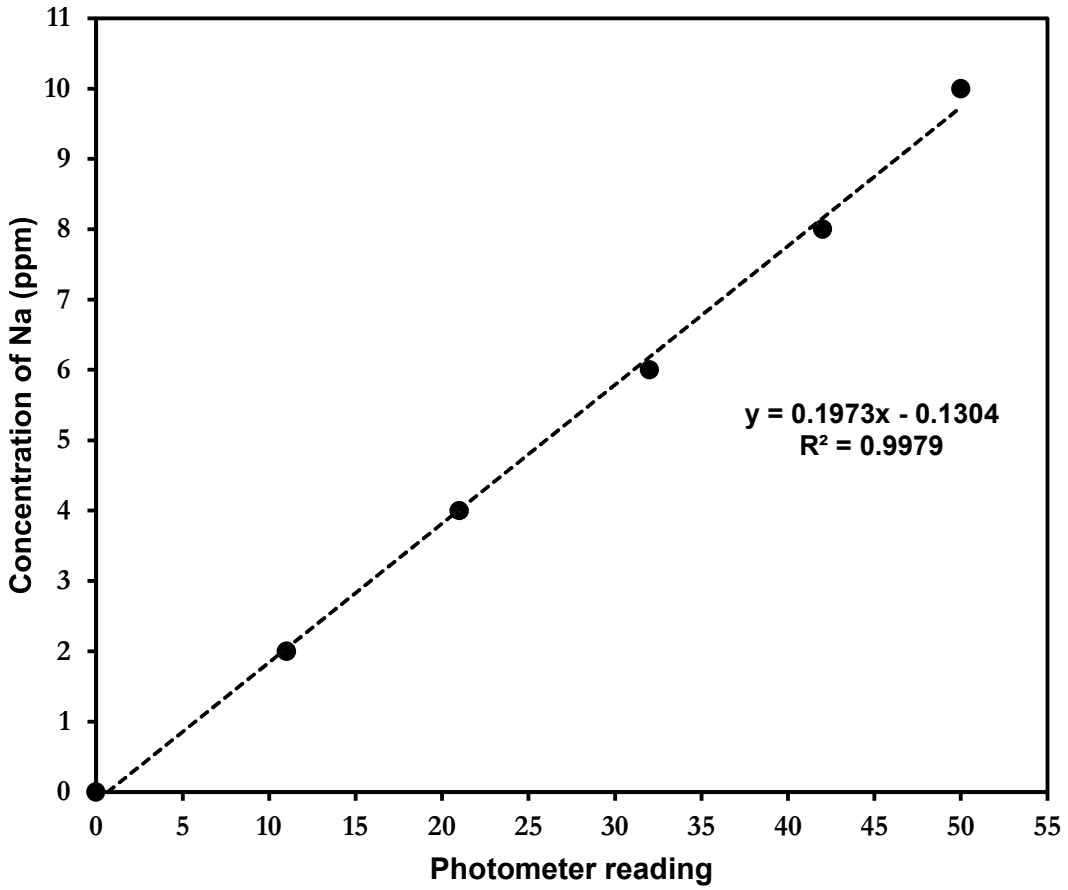

Figure 4.4: Calibration curve of concentration of Na against intensity of flame photometer readings

Table 4.5: Cation exchange capacity of diatomite from 4 trials

Trial	[Na+] in the sample, (mg/L)	[Na+] in the blank, (mg/L)	[Na+] after correction, (mg/L)	CEC (meq/100g)
1	83.54	1.64	81.9	8.91
2	77.62	1.64	75.98	8.26
3	65.78	1.64	64.14	6.97
4	71.7	1.64	70.06	7.62
				$\bar{x}$ **=7.94**
				σ **=0.83**

4.7 Sorption capacity of diatomite samples

The study for the sorption capacity of diatomite involved equilibrating diatomite with the simulated liquid waste solution containing known concentrations of Co, Zn and Ba ions. The quantities of Co, Zn and Ba in mg were determined by subtracting the final concentrations of Co, Zn and Ba from their corresponding initial concentration before contact with the diatomite sorbent and multiplying the result by batch volume of 0.1 litres. The study investigated the effect of sorbent concentration, initial concentration of metal cations, pH and the contact time.

4.7.1 Variation of removal of ions with sorbent concentration

Table 4.6 shows the results of the study on the effect of adsorbent contents.

Figure 4.5 shows the variation of sorption efficiency with diatomite content.

These results show that the adsorption efficiency of Co, Zn and Ba was enhanced as the amount of the adsorbent was increased between 0.5 g per 100 ml and 3.0 g per 100 ml. This trend is explained by the fact that an increase in diatomite content, while retaining the initial concentrations of Co, Zn and Ba results raises the ratio of the number of sorption sites to the number of ions of Co, Zn and Ba. At low diatomite dose, all adsorption sites come in contact with metal ions, and the surface reaches saturation more quickly, whereas at high diatomite content, many sites are available for Co, Zn, and Ba sorption. The same trend was observed by other studies, such that by; Ibrahim et al (2013), Sheng et al (2008), ElSayed et al (2018) and Salman et al (2016) who studied the influence of diatomite content on adsorption of the target cations.

The selectivity sequence depicted from the graph in Figure 4.5 is given as $Zn > Co > Ba$. This is due to the relationship between heavy metal ionic radii and diatomite external and internal pore diameters. Since diatomite has a positive surface charge, electronegativity and ionic radius of the target ion in a multi-metal solution influence its position in the selectivity sequence.

The comparison of ionic radius and electronegativity of Zn, Co and Ba is as displayed in Table 4.7. The Table 4.7 shows that Zn has the highest ratio of electronegativity to ionic radius while Ba has the least. The ratio of electronegativity to ionic radius for Co is intermediate between that of Zn and Ba hence the sorption selectivity sequence depicted from the graph in figure 4.5 given as $Zn > Co > Ba$ indicates that the ratio of electronegativity to ionic radius decreases down the selectivity sequence. The selectivity sequence observed in this study is in agreement with the results obtained in a similar study by Elyased (2017) which placed Zn ahead of Ba in the sorption selectivity sequence.

Table 4.6: The variation of removal of Co, Zn and Ba ions with the diatomite concentration

Diatomite Concentration (g /100 ml)	Co			Zn			Ba		
	C_i (mg/L)	C_t (mg/L)	η (%)	C_i (mg/L)	C_t (mg/L)	η (%)	C_i (mg/L)	C_t (mg/L)	η (%)
0.5	13.431	3.756	72.04	12.668	0.667	94.74	12.647	9.619	23.95
1.0	13.431	2.646	80.30	12.668	0.243	98.09	12.647	8.714	31.10
1.5	13.431	2.096	84.39	12.668	0.198	98.44	12.647	6.682	47.17
2.0	13.431	2.046	84.77	12.668	0.166	98.69	12.647	5.657	55.27
2.5	13.431	0.986	92.66	12.668	0.051	99.60	12.647	1.815	85.65
3.0	13.431	1.403	89.55	12.668	0.022	99.83	12.647	1.856	85.33

Table 4.7: Comparison of Ionic radius and electronegativity of Zn, Co and Ba

Metal	Ionic radius (pm)	Electronegativity (Linus Pauling Scale)	$\frac{Electronegativity}{IonicRadius}$
Zn	139	1.65	0.127
Co	200	1.88	0.009
Ba	268	0.89	0.003

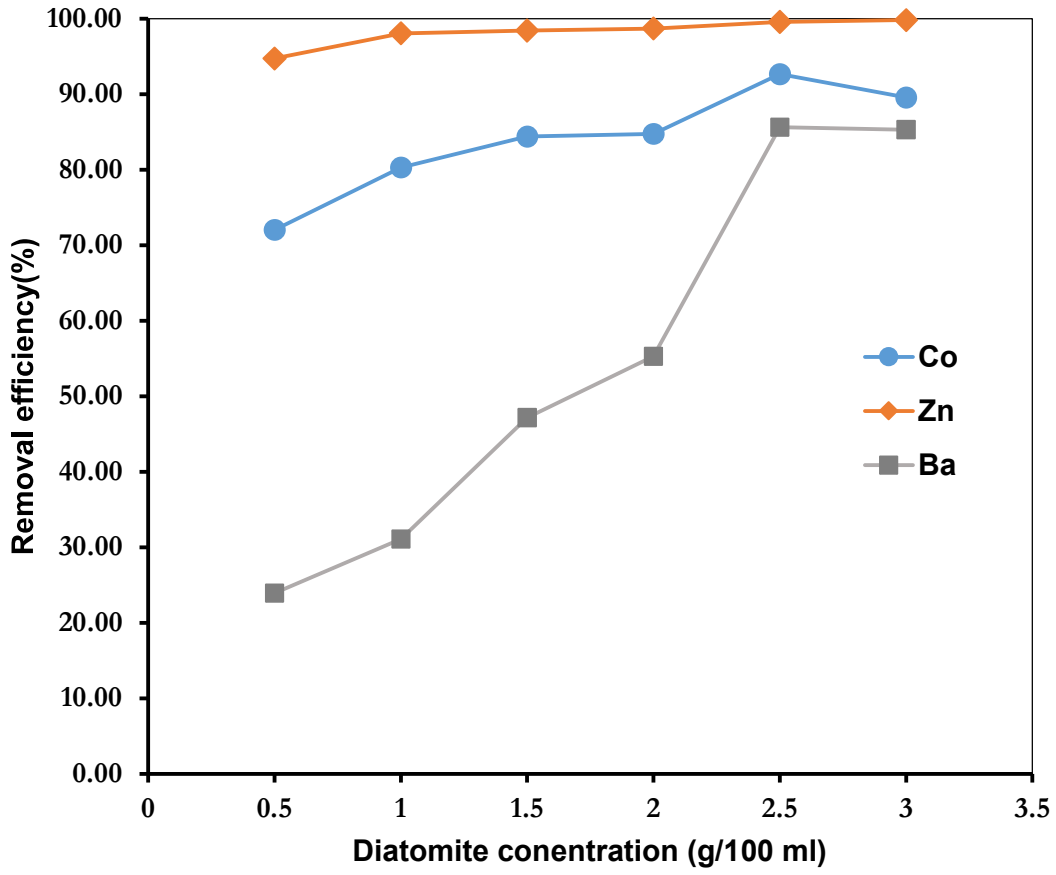

Figure 4.5: Variation of the removal of Ba, Zn and Co ions with diatomite concentration

While it has been established from figure 4.5 that the adsorption percentage of diatomite for Co, Zn and Ba was enhanced with increase in the diatomite concentration, it will be inadequate to only judge the potential of an adsorbent based on the adsorption percentage alone. For instance, it will not be necessarily correct to conclude that the diatomite concentration with the highest adsorption percentage corresponds to the optimum content. It is possible that the additional diatomite brings about an increase in the removal efficiency yet we end up with a relatively higher proportion of vacant adsorption sites than before. Hence it is critical, as well, to monitor the effect of increasing diatomite concentration on the adsorption capacity of diatomite for Co, Zn and Ba. Table 4.8 and figure 4.6 shows the effect of increasing diatomite concentration on the adsorption capacity of diatomite for Co, Zn and Ba. As we can see from figure 4.6, the adsorption capacity of diatomite for Co, Zn and Ba was reduced when the diatomite concentration was increased from 0.5 g per 100 ml to 3.0 g per 100 ml. The decline in the adsorption capacity with increase in diatomite concentration is attributed to underutilization of adsorption sites. Even though the adsorption percentage is higher for higher diatomite content, the quantity of target metals removed per unit weight of the adsorbent is smaller due to unused adsorption sites.

Table 4.8: The variation of removal of Co, Zn and Ba ions with diatomite concentration

Diatomite conc. (g/100 ml)	Co			Zn			Ba		
	C_i (mg/L)	C_t (mg/L)	q_m (mg/g)	C_i $(m\ /L)$	C_t $(m\ /L)$	q_m (mg/g)	C_i (mg/L)	C_t (mg/L)	q_m (mg/g)
0.5	13.431	3.756	1.94	12.668	0.667	2.40	12.647	9.619	0.61
1	13.431	2.646	1.08	12.668	0.243	1.24	12.647	8.714	0.39
1.5	13.431	2.096	0.76	12.668	0.198	0.83	12.647	6.682	0.40
2	13.431	2.046	0.57	12.668	0.166	0.63	12.647	5.657	0.35
2.5	13.431	0.986	0.50	12.668	0.051	0.50	12.647	1.815	0.43
3	13.431	1.403	0.40	12.668	0.022	0.42	12.647	1.856	0.36

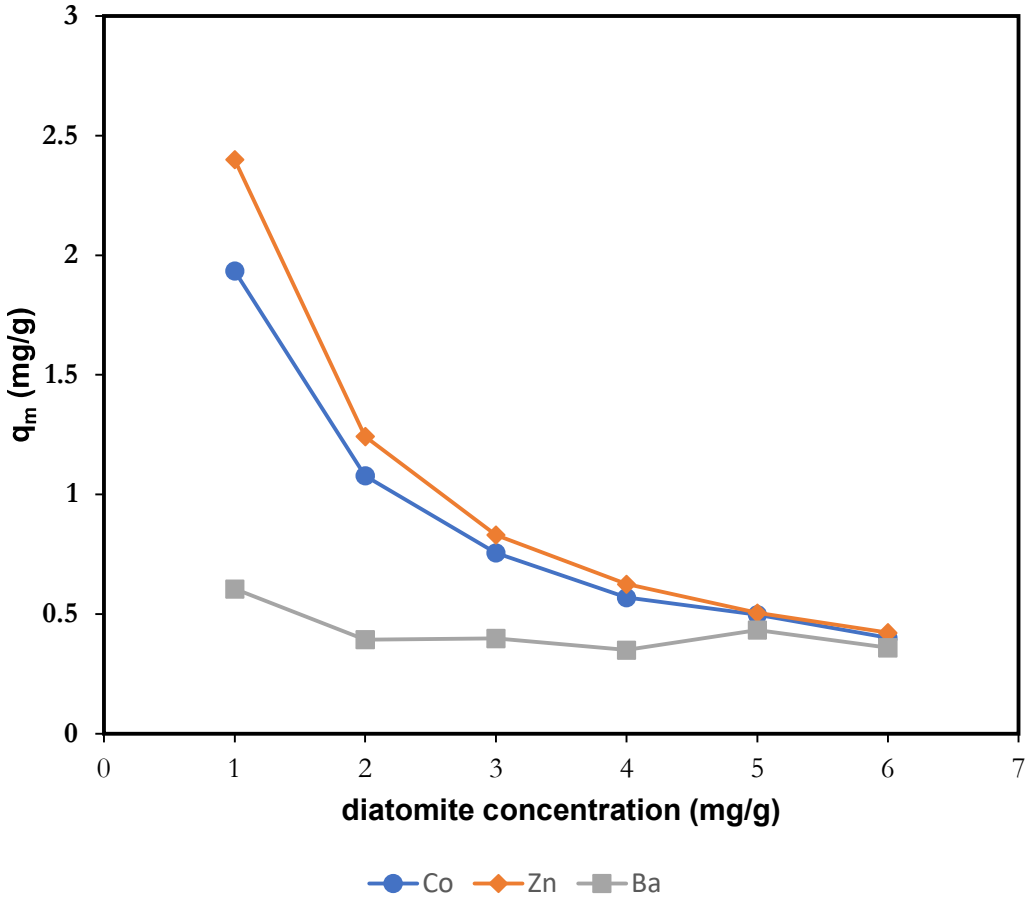

Figure 4.6: Variation of removal of Ba, Zn and Co ions with of diatomite concentration

4.7.2 Variation of removal of Co, Zn and Ba ions with the initial metallic concentration

To examine the variation of removal of Co, Zn and Ba ions with the initial concentration of Co, Zn and Ba, the concentrations of Co, Zn and Ba were halved in each of the four subsequent runs by diluting the prepared simulated waste solution containing 7.458 mg/L of Co, 8.289 mg/L of Zn and 10.662 mg/L of Ba with double distilled water. At each initial metallic concentration, the simulated solution was contacted with 2.0 g diatomite per 100 ml, 2.5 diatomite per 100 ml and 3.0 g diatomite per 100 ml. The pH and the contact time were held constant at 6 and 4 hours respectively.

4.7.2.1 Variation of removal of Co, Zn and Ba ions with initial metallic concentration

The data from the study on the variation of sorption of Co, Zn and Ba ions from solution with initial metallic concentrations are presented in Table 4.9, Table 4.10 and figure 4.7 to figure 4.10.

In general, the total adsorption capacity for the Co, Zn and Ba increases when the initial concentrations are increased. Increasing the initial metallic concentration increases the difference in concentration between the active sites of diatomite surface and the aqueous metallic solution. As the difference in the concentration between the adsorbent and the adsorbate grows, so does the driving force for mass transfer between the metallic aqueous solution and the diatomite surface. The increase in the initial concentrations, as well, increases the number of cobalt (II), zinc (II) and barium (II) ions available to the binding sites of the diatomite sorbent. Hence increasing the initial metallic concentrations enhances the adsorption capacity of diatomite for Co, Zn and Ba. This trend is consistent with the results from the study by Yusan et al (2012) on the effect of the initial concentration of Th (IV); Calsikan et al (2011) on the role of initial concentration of Zn (II) ions on adsorption capacity of diatomite; and Iran et al (2011) on the role of the initial concentration of lead ions on the capacity of diatomite to adsorb lead ions.

Figure 4.7 shows that the increase in diatomite content was observed to reduce the adsorption capacity of diatomite. When the initial concentrations are between 4 and 8 times of the initial metallic concentrations, the adsorption capacity of diatomite appears to be independent of the level of diatomite content. The decrease in adsorption capacity following the increase in diatomite content occurred because the available sorption sites were not fully utilized at a higher adsorbent content as compared to lower adsorbent content.

The effect of initial metallic concentration on the adsorption efficiency indicated a different pattern from that on the adsorption capacity. Figure 4.8 and figure 4.9 show that, when the initial concentrations of Co and Zn were decreased, the removal efficiencies of Co and Zn were observed to increase. This is because decreasing the initial cation concentrations at constant adsorbent dosing reduces the number of cations per unit volume that require diatomite adsorption sites. At low initial concentrations a higher proportion of the Co and Zn ions find binding sites on the diatomite hence the high removal efficiency. A similar trend was observed by Nenadovic et al (2015) on the effect of initial Cs concentration on the immobilization efficiency of Cs by diatomite sorbent.

The effect of the initial concentration of Ba on its removal efficiency gave a different trend as shown in figure 4.10, from that of Zn and Co. Barium registered a decline in removal efficiency when its initial concentration was decreased from 10.7 mg/L to 2.7 mg/L, whereas an increase in removal efficiency was observed when its initial concentration was decreased from 2.7 mg/L to 0.7 mg/L.

Table 4.9: The variation of sorption of Co, Zn and Ba ions from solution with initial metallic concentrations

Diat cont. (g)	Co			Zn			Ba		
	C_i (mg/L)	C_t $(m\ \ /L)$	η (%)	C_i (mg/L)	C_t (mg/L)	η (%)	C_i (mg/L)	C_t (mg/L)	η (%)
2.0	7.458	7.160	4.00	8.289	6.055	26.95	10.662	0.934	91.24
2.0	3.729	3.471	6.92	4.144	1.749	57.81	5.331	1.677	68.54
2.0	1.865	1.328	28.80	2.072	0.382	81.57	2.665	1.515	43.18
2.0	0.932	0.286	69.32	1.036	0.046	95.61	1.333	0.535	59.86
2.0	0.466	0.107	77.12	0.518	0.022	95.75	0.666	0.142	78.69
2.5	7.458	6.914	7.30	8.289	4.915	40.70	10.662	0.891	91.65
2.5	3.729	2.978	20.15	4.144	1.305	68.52	5.331	1.360	74.49
2.5	1.865	0.838	55.08	2.072	0.141	93.22	2.665	1.331	50.08
2.5	0.932	0.099	89.38	1.036	0.041	96.09	1.333	0.365	72.61
2.5	0.466	0.033	92.92	0.518	0.033	93.63	0.666	0.066	90.10
3.0	7.458	6.841	8.27	8.289	3.857	53.47	10.662	0.611	94.27
3.0	3.729	2.559	31.39	4.144	0.666	83.94	5.331	0.957	82.05
3.0	1.865	0.599	67.90	2.072	0.091	95.63	2.665	0.853	68.02
3.0	0.932	0.043	95.39	1.036	0.020	98.12	1.333	0.322	75.84
3.0	0.466	0.004	99.14	0.518	0.030	94.14	0.666	0.052	92.20

Table 4.10: The variation of sorption of Co, Zn and Ba ions from solution with initial metallic concentrations

Diatomite dose (g)	Initial concentration	Co $q_t \times 10^{-6}$ (mol/g)	Zn $q_t \times 10^{-6}$ (mol/g)	Ba $q_t \times 10^{-6}$ (mol/g)	Total $q_t \times 10^{-6}$ (mol/g)
2.0	Ci	0.305	0.379	0.191	0.875
2.0	2Ci	0.548	0.757	0.290	1.596
2.0	4Ci	0.456	1.292	0.419	2.167
2.0	8Ci	0.219	1.832	1.330	3.381
2.0	16Ci	0.253	1.708	3.542	5.503
2.5	Ci	0.294	0.297	0.175	0.766
2.5	2Ci	0.566	0.609	0.282	1.456
2.5	4Ci	0.697	1.181	0.389	2.267
2.5	8Ci	0.510	1.737	1.157	3.404
2.5	16Ci	0.369	2.063	2.846	5.278
3.0	Ci	0.261	0.249	0.149	0.659
3.0	2Ci	0.503	0.518	0.245	1.266
3.0	4Ci	0.716	1.010	0.440	2.166
3.0	8Ci	0.662	1.773	1.062	3.497
3.0	16Ci	0.349	2.259	2.440	5.047

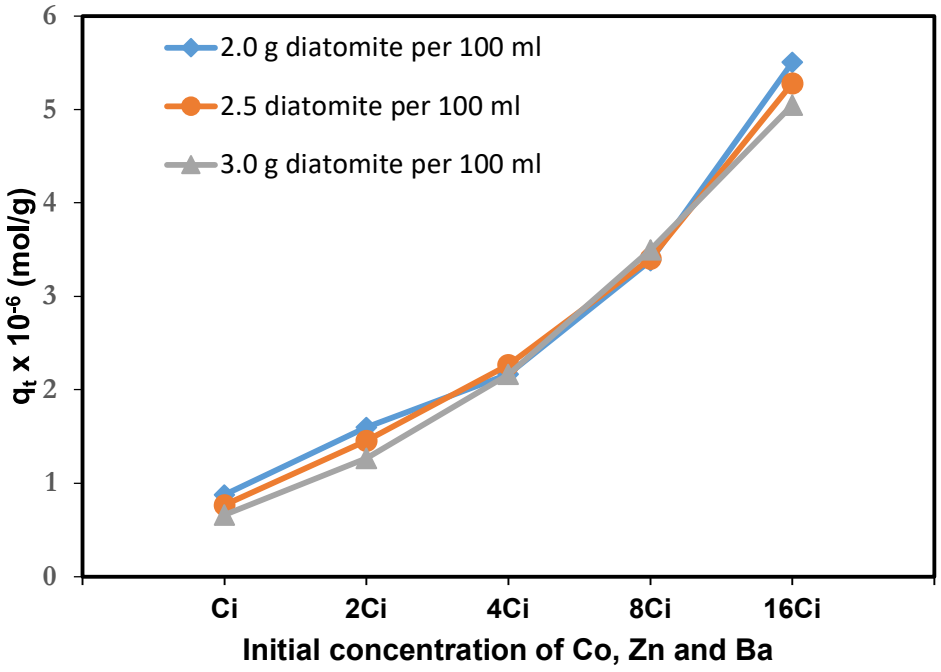

Figure 4.7: The variation of removal of Co, Zn and Ba ions from solution with initial metallic concentrations and diatomite content

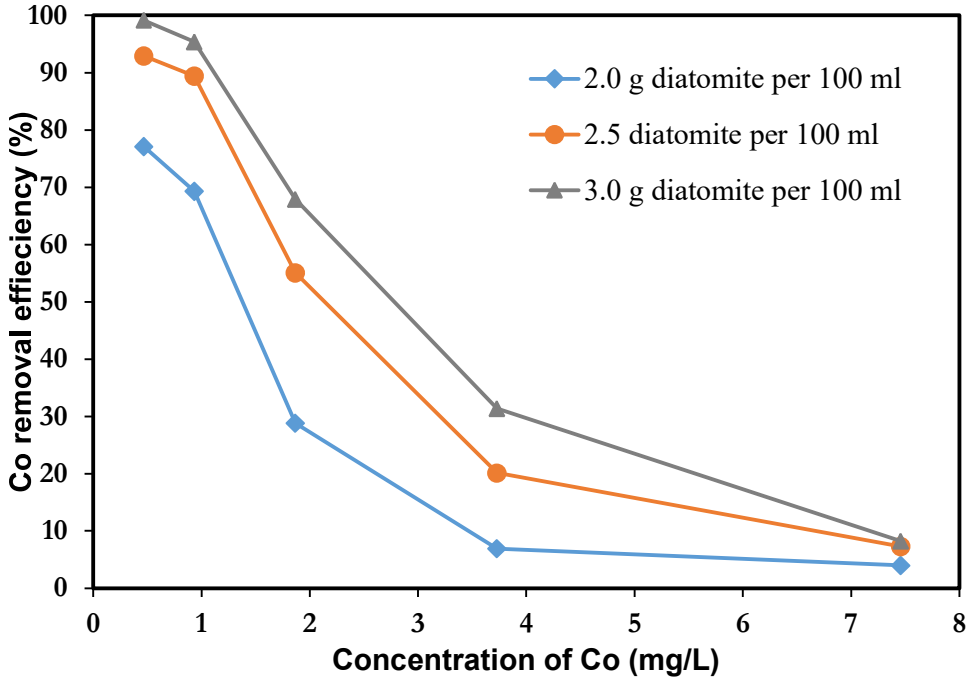

Figure 4.8: The variation of removal efficiency of Co ions from solution with initial metallic concentrations and diatomite content

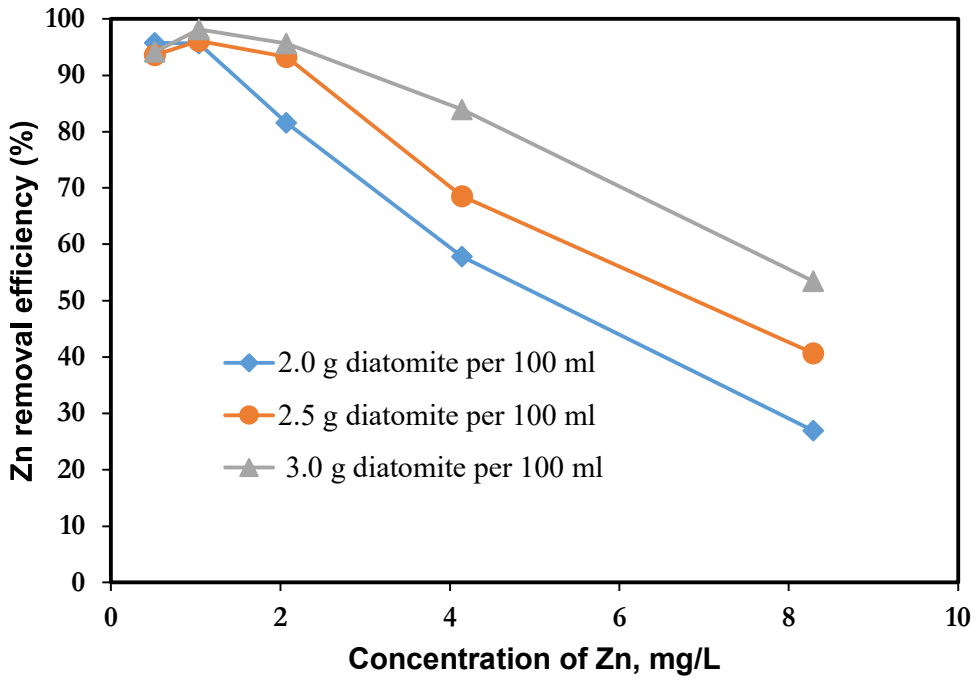

Figure 4.9: The variation of removal efficiency of Zn ions from solution with initial metallic concentrations and diatomite content

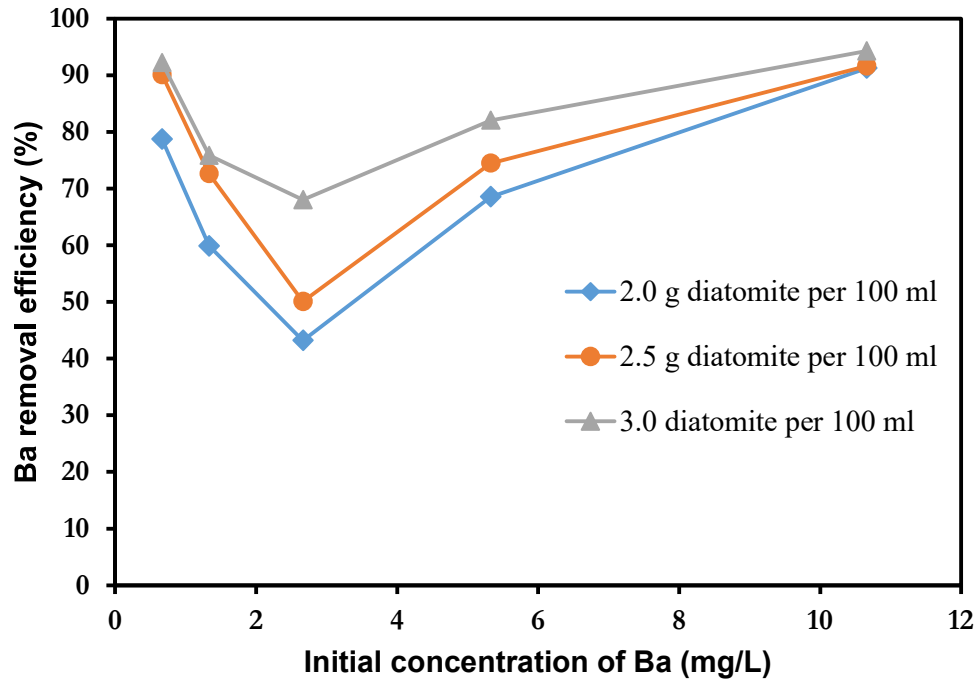

Figure 4.10: The variation of sorption efficiency of Ba ions from solution with initial metallic concentrations and diatomite content

Data obtained on the effect of initial concentration of Co, Zn and Ba show that, initially, Ba is preferentially adsorbed over both Co and Zn. The apparent preference of Ba was attributed to its initial concentration being considerably higher than that of both Co and Zn. As the initial concentrations of Ba, Co and Zn was halved in subsequent runs, the differences in the initial concentrations of Ba, Co and Zn become smaller and smaller hence barium progressively lost its competitive edge over Co and Zn.

The initial decline in removal efficiency of Ba as its initial concentration is reduced is caused by the reposition from the top of adsorption sequence to the bottom as it continually reduces its competitive advantage in the subsequent runs. Once Ba has repositioned itself at the bottom of the adsorption sequence, its removal efficiency is observed to increase with decrease in its initial concentration as expected.

4.7.2.2 The variation of the adsorption capacity of diatomite with initial metallic concentration of Co, Zn and Ba ions

So as to determine the effect of initial concentration on the adsorption capacity of diatomite for Co, Zn and Ba from multicomponent solution, the data in Table 4.9 on initial and final concentrations of Co, Zn and Ba was used to calculate the respective adsorption capacities and the results are as presented in Table 4.11. The adsorption capacity was plotted against the initial concentration for diatomite content of 2.0 per 100 ml, 2.5 g per 100 ml and 3.0 g per 100 ml as presented in figures 4.11, 4.12 and 4.13 respectively.

From figure 4.11, 4.12 and 4.13, the adsorption capacity of diatomite for Co increases as the initial concentration is doubled for the first three datapoints but then reduces for the next two subsequent datapoints. For the case of Zn, the adsorption capacity increases as its initial concentration in the solution is doubled and appears to approach a constant value. For both Co and Zn, the increase in adsorption capacity is characterized by curve whose gradient decreases with increase in concentration. This implies that the increase on adsorption capacity with increase in concentration occurs at a decreasing rate. This trend can be explained from the understanding that, an increase in initial concentration increases the number of target cations that interact with the active sites of the diatomite sorbent. As the initial concentration is increased further with other parameters held constant, the active sites get saturated faster and once almost all the sites have been occupied the adsorption capacity approaches a constant value in the case of a single component adsorption system. The variation of the adsorption capacity of Zinc with its initial concentration in the multicomponent system is identical to that

of single solute systems. For the case of Co, however, the adsorption capacity starts to decrease instead of approaching a constant value. For Ba on the other hand, the adsorption capacity increases with increasing concentration at an increasing rate. The deviation of the trends of Co and Ba from those of single solute systems arises as a result of competition of target cations for the binding spaces on the diatomite sorbent.

Table 4.11: The variation of the adsorption capacity of diatomite with initial metallic concentration of Co, Zn and Ba ions

Diat cont. (g)	Co			Zn			Ba		
	C_i (mg/L)	C_t (mg/L)	$q_{t,Co}$ $*10^{-2}$ (mg/g)	C_i $(m\ /L)$	C_t $(m\ /L)$	$q_{t,Zn}$ $*10^{-2}$ $(m\ /g)$	C_i (mg/L)	C_t (mg/L)	$q_{t,Ba}$ $*10^{-2}$ (mg/g)
2	7.458	7.16	1.49	8.289	6.055	11.17	10.662	0.934	48.64
2	3.729	3.471	1.29	4.144	1.749	11.98	5.331	1.677	18.27
2	1.865	1.328	2.69	2.072	0.382	8.45	2.665	1.515	5.75
2	0.932	0.286	3.23	1.036	0.046	4.95	1.333	0.535	3.99
2	0.466	0.107	1.80	0.518	0.022	2.48	0.666	0.142	2.62
2.5	7.458	6.914	2.18	8.289	4.915	13.50	10.662	0.891	39.08
2.5	3.729	2.978	3.00	4.144	1.305	11.36	5.331	1.36	15.88
2.5	1.865	0.838	4.11	2.072	0.141	7.72	2.665	1.331	5.34
2.5	0.932	0.099	3.33	1.036	0.041	3.98	1.333	0.365	3.87
2.5	0.466	0.033	1.73	0.518	0.033	1.94	0.666	0.066	2.40
3	7.458	6.841	2.06	8.289	3.857	14.77	10.662	0.611	33.50
3	3.729	2.559	3.90	4.144	0.666	11.59	5.331	0.957	14.58
3	1.865	0.599	4.22	2.072	0.091	6.60	2.665	0.853	6.04
3	0.932	0.043	2.96	1.036	0.02	3.39	1.333	0.322	3.37
3	0.466	0.004	1.54	0.518	0.03	1.63	0.666	0.052	2.05

In a multicomponent competitive adsorption system, the cations in the simulated liquid waste compete for space on the active sites of the sorbent. The highly competitive species will displace the less competitive species from the binding space on the sorbent. However, the less competitive species may also displace the highly competitive species if their concentration in the multicomponent system is sufficiently higher.

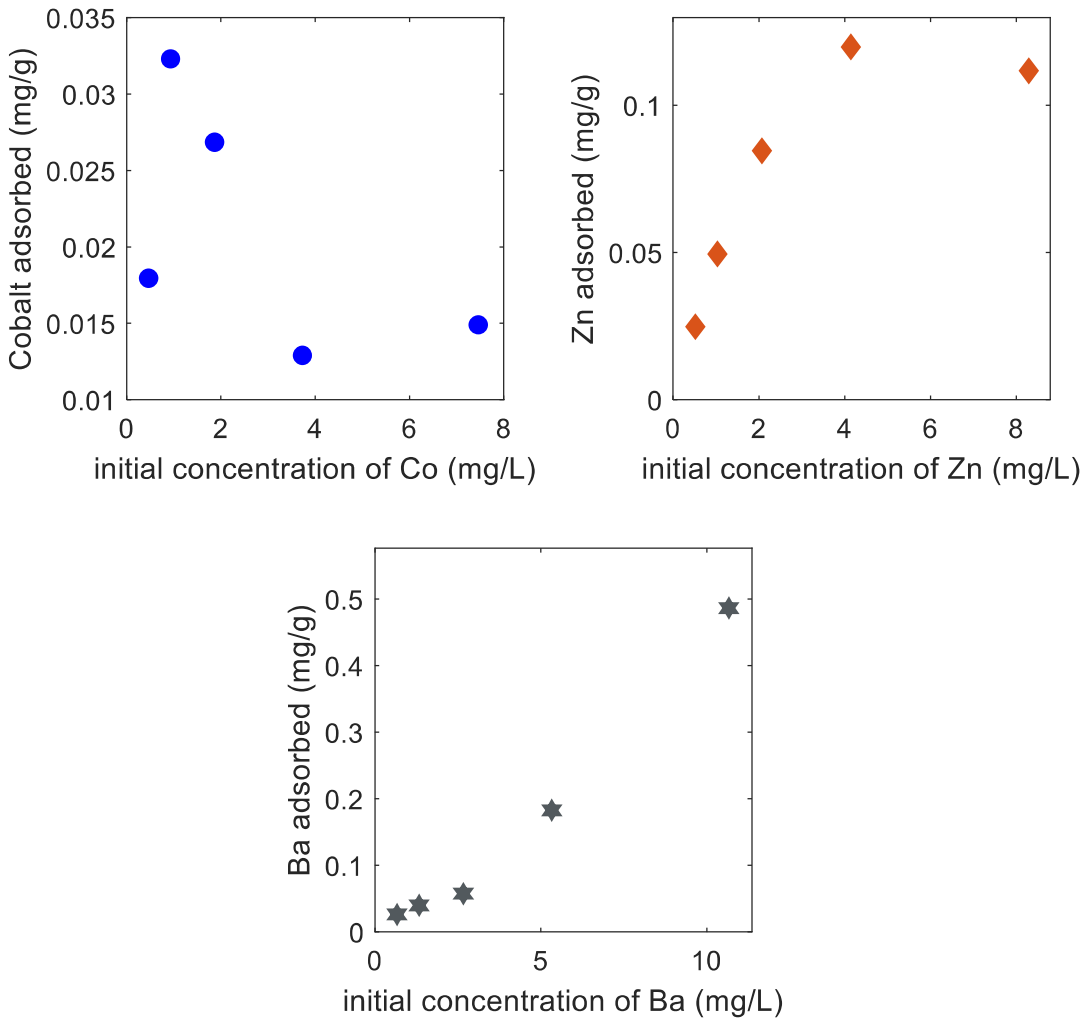

Figure 4.11: The variation of the adsorption capacity of diatomite with initial metallic concentration of Co, Zn and Ba ions at a diatomite content of 2.0 g per 100 ml

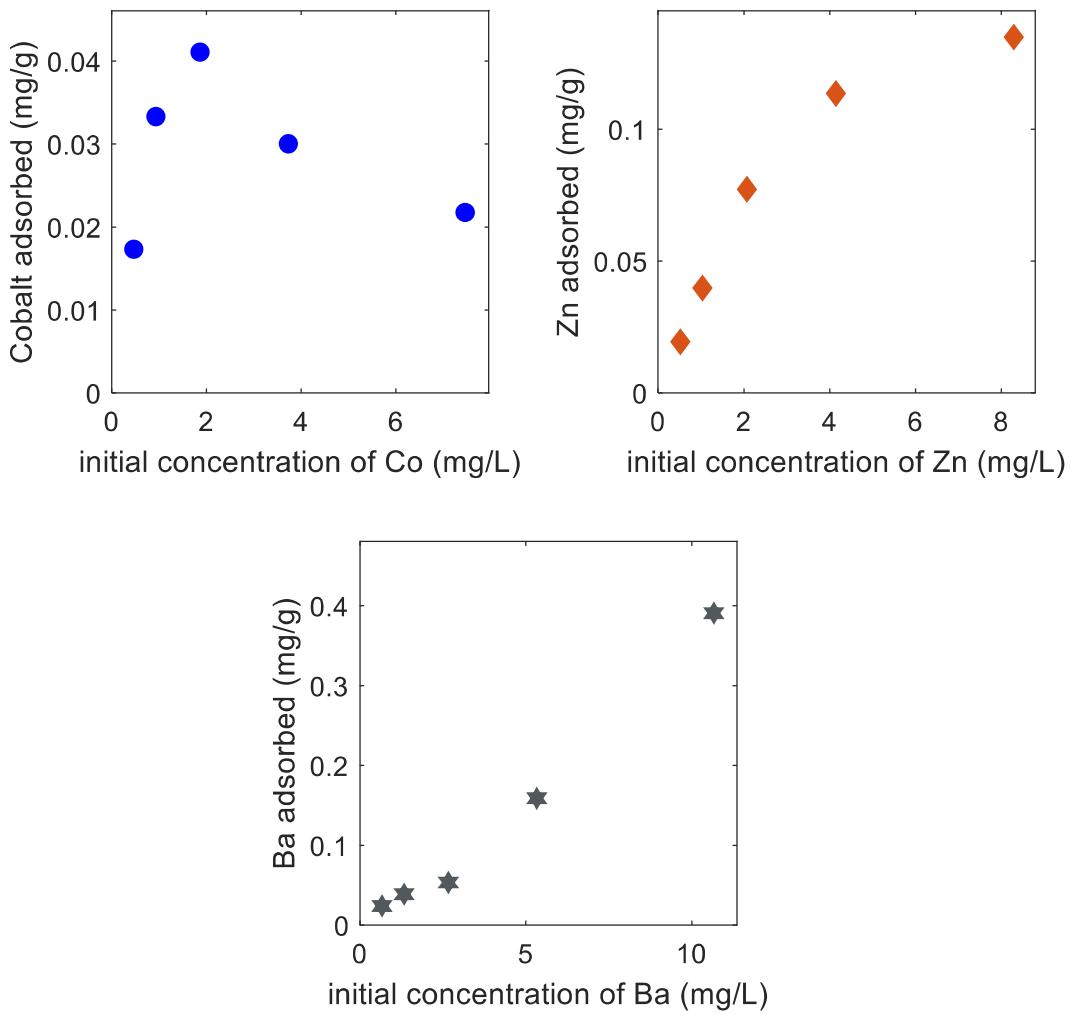

Figure 4.12: The variation of the adsorption capacity of diatomite with initial metallic concentration of Co, Zn and Ba ions at a diatomite content of 2.5 g per 100 ml

In the context of a Co, Zn and Ba multicomponent system, the selectivity sequence was established to be Zn>Co>Ba and this was explained by the trend in the ratio of electronegativity to ion radius as presented in Table 4.9. This means that Zn ions is the species that interacts with binding sites the strongest of three cations while Ba ions is the species that interact with binding sites the weakest of the three cations. As can be seen from the figure 4.11, 4.12 and 4.13, Zn is competitive enough such that its plot of adsorption capacity assumes a shape that is much closer to that would take if it was adsorbed from a single component solution.

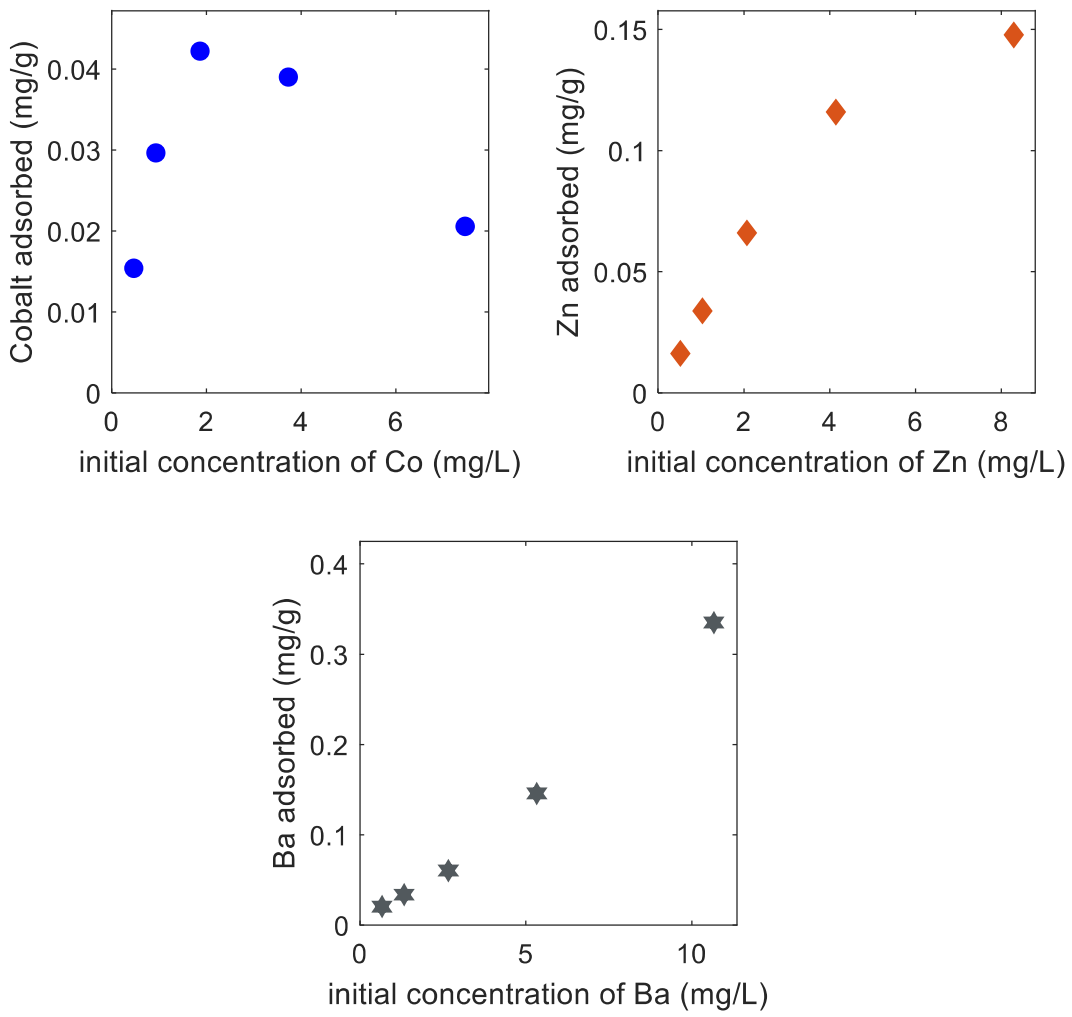

Figure 4.13: The variation of the adsorption capacity of diatomite with initial metallic concentration of Co, Zn and Ba ions at a diatomite content of 3.0 g per 100 ml

Note that the initial concentrations of Co, Zn and Ba of 0.466 mg/L ,0.518 mg/ and 0.666 mg/L respectively show that Ba concentration was higher than that of both Co and Zn. As the initial concentrations were doubled, the more the Ba gained advantage in terms of the numbers of its ions interacting with the binding sites. This explain the reason why its adsorption capacity curve rises at an increasing rate as the initial metallic concentrations are doubled. For Co, the first three datapoints show a curve that resembles the shape that it would assume if it were adsorbed from a single component solution. However, for the last two datapoints, the Ba

appears to have gained an upper hand over Co due its higher initial concentration. This explains why the adsorption capacity of Co decreases for the last two datapoints.

As the initial concentrations are doubled, the Ba's concentration advantage over both Co and Zn doubles. Since Zn is the most competitive followed by Co, the effect of doubling the concentration advantage of Ba is first felt on Co and then Zn. As it can be seen from figure 4.11, the last three datapoints on the Co plot indicate a decline in adsorption capacity while for Zn it is only the last data point that shows a decline in adsorption capacity. This implies the effect of doubling Ba concentration advantage is more felt on Co than Zn. The comparison of the plots in figure 4.11, 4.12 and 4.13 indicates that the effect of doubling the concentration advantage of Ba reduces as the diatomite content was increased from 2.0 g per 100 ml to 3.0 g per 100 ml. This can be explained by the fact that as the diatomite content is increased, the number of bindings sites increases and this reduces the competition among Co, Zn and Ba ions for available binding spaces on the diatomite sorbent.

4.7.3 Variation of removal of Co, Zn and Barium ions with contact time

Table 4.12 and figure 4.14 shows the results of the effect of varying contact time, while holding diatomite content, pH and initial concentrations constant. Table 4.13 and figure 4.15 shows data and the plot on the impact that varying contact of simulated waste has on the amount of Co, Zn and Ba adsorbed by diatomite per unit mass of the diatomite sorbent.

In general, the removal efficiency increases as the time allowed for adsorption is increased. After 5 hours of contact between the diatomite sorbent and the simulated waste solution, there was no appreciable increase in adsorption efficiency with the increase in time. As more contact time is allowed, the mass transfer of cations from the solution to the binding sites occurs until an equilibrium between the adsorbent and adsorbent is reached. Beyond the point of equilibrium, allowing more contact time between diatomite sorbent and Co, Zn and Ba does not yield any appreciable change in the percentage removal efficiency. Similarly, beyond the point of equilibrium, there is no appreciable change in the amount adsorbed per unit mass of the diatomite sorbent.

Table 4.12: Variation of removal of Co, Zn and Barium ions with contact time

	Co			Zn			Ba		
Time (hrs)	C_i (mg/L)	C_t (mg/L)	η (%)	C_i (mg/L)	C_t $(m\ /L)$	η (%)	C_i (mg/L)	C_t (mg/L)	η (%)
1	7.458	6.923	7.17	8.289	4.780	42.33	10.662	2.826	73.50
2	7.458	6.355	14.79	8.289	4.679	43.55	10.662	1.874	82.43
3	7.458	5.910	20.75	8.289	4.143	50.02	10.662	0.757	92.90
4	7.458	5.683	23.80	8.289	4.004	51.69	10.662	0.619	94.19
5	7.458	4.848	34.99	8.289	2.934	64.60	10.662	0.573	94.63
6	7.458	4.867	34.74	8.289	3.01	63.69	10.662	0.236	97.79

Table 4.13: The variation of the amount of Co, Zn and Ba ions adsorbed on diatomite per unit mass of diatomite with contact time

	Co			Zn			Ba		
Time (hrs)	C_i (mg/L)	C_t (mg/L)	q_t (mg/g)	C_i (mg/L)	C_t (mg/L)	q_t (mg/g)	C_i (mg/L)	C_t (mg/L)	q_t (mg/g)
1	7.458	6.923	0.021	8.289	4.780	0.140	10.662	2.826	0.313
2	7.458	6.355	0.044	8.289	4.679	0.144	10.662	1.874	0.352
3	7.458	5.910	0.062	8.289	4.143	0.166	10.662	0.757	0.396
4	7.458	5.683	0.071	8.289	4.004	0.171	10.662	0.619	0.402
5	7.458	4.848	0.104	8.289	2.934	0.214	10.662	0.573	0.404
6	7.458	4.867	0.104	8.289	3.010	0.211	10.662	0.236	0.417

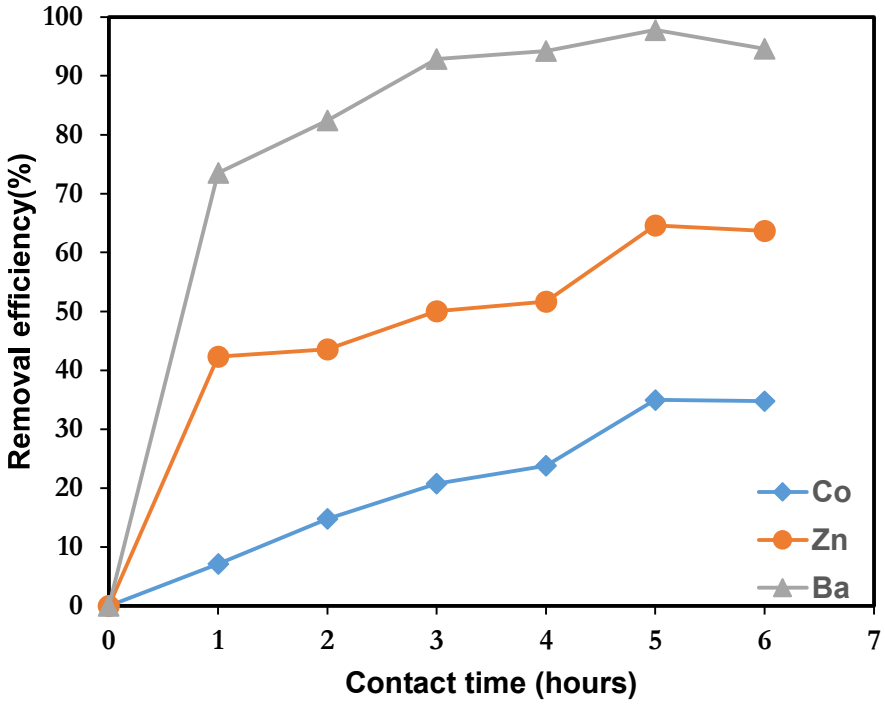

Figure 4.14: Variation of removal of Co, Zn and Barium ions with contact time

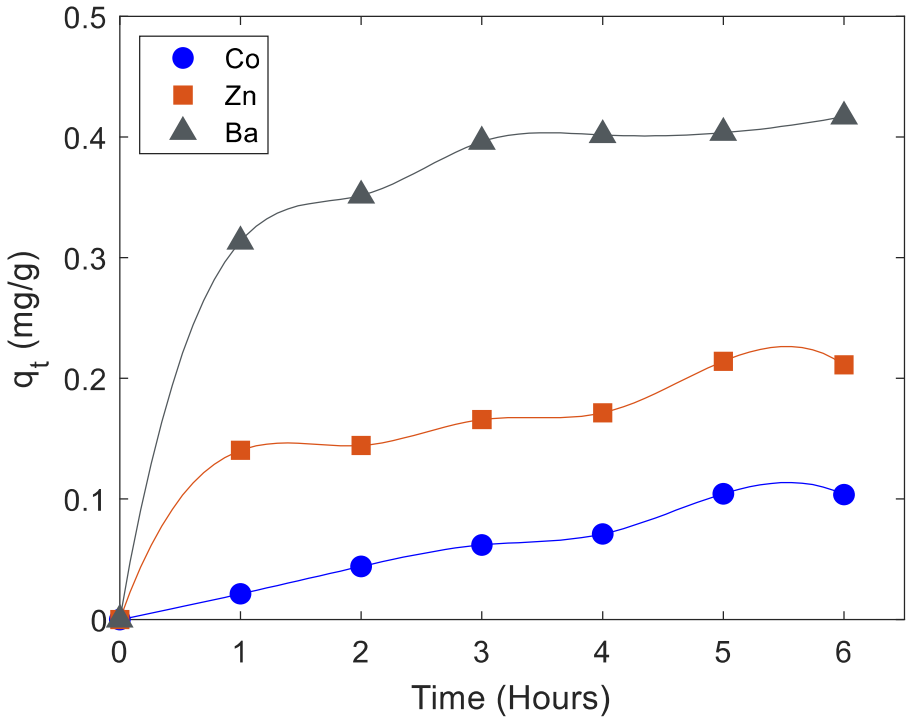

Figure 4.15: The variation of amount of Co, Zn and Ba ions adsorbed on diatomite per unit mass of diatomite with contact time

4.7.4 The variation of removal efficiency of Co, Zn and Ba ions with pH

Table 4.14 and figure 4.16 shows data and the plot on the variation of removal of Co, Zn and Ba ions with pH. Table 4.15 and figure 4.17 shows data and the plot on the variation of the amount of Co, Zn and Ba adsorbed by diatomite per unit mass of the diatomite sorbent with pH.

The adsorption efficiency of diatomite is observed to increase as the pH of solution is increased. This can be explained by changes in the surface charge of diatomite when the pH is varied. The surface of diatomite becomes positively charged for the pH values lower than the Point of Zero Charge (PZC), neutral when the pH is equal to the PZC, and negatively charged for pH values higher than the PZC. At pH < PZC, the protonation of $SiOH$ takes precedence rendering the diatomite surface positive, whereas at pH > PZC, the deprotonation $SiOH$ takes precedence rendering the surface of diatomite negative as shown in the following reactions:

$$Protonation: \equiv SiOH + H^+ \rightarrow \equiv SiOH_2^+$$

$$Deprotonation: \equiv SiOH \rightarrow \equiv SiO^- + H^+$$

Where ≡ denotes the surface of diatomite.

The uptake of metal ions by diatomite is enhanced when the diatomite surface charge is opposite to that of the metal cations such that the cations are electrostatically attracted on the diatomite surface. As the pH rises above 2, the positive charge density on the surface of diatomite decreases until PZC, at which point the negative charge density rises. As the pH is raised beyond the point PZC, electrostatic forces of attraction between metal ions and surface of diatomite are enhanced, resulting in an increase in the rate of adsorption.

At pH greater than 7, precipitations of Ba, Zn and Co occurs when NaOH drops are added to adjust the pH. During filtration, the precipitated Ba, Zn and Co are retained as a residue on the filter paper and could be falsely interpreted as having been adsorbed by diatomite. The apparent surge in adsorption efficiency at PH greater than 7 is therefore a joint effect of precipitation and adsorption. As it can be seen in figure 4.16 and figure 4.17, the trend of the impact of pH on the removal efficiency of Co, Zn and Ba is similar to that of the impact of pH on the amount adsorbed per unit mass of the diatomite sorbent.

Table 4.14: The variation of removal efficiency of Co, Zn and Ba ions with pH

	Co			Zn			Ba		
pH	C_i (mg/L)	C_t (mg/L)	η (%)	C_i (mg/L)	C_t $(m\ \ /L)$	η (%)	C_i $(m\ \ /L)$	C_t $(m\ \ /L)$	η (%)
2	5.999	5.653	5.77	5.982	5.314	11.17	6.877	4.686	31.87
4	5.999	5.247	12.54	5.982	4.077	31.85	6.877	0.729	89.40
6	5.999	4.970	17.15	5.982	3.170	47.00	6.877	0.513	92.53
8	5.999	1.244	79.27	5.982	0.077	98.71	6.877	0.717	89.57
10	5.999	0.006	99.91	5.982	0.014	99.77	6.877	0.450	93.46

Table 4.15: The variation of the amount of Co, Zn and Ba adsorbed on diatomite per unit mass of diatomite with the pH

	Co			Zn			Ba		
pH	C_i (mg/L)	C_t (mg/L)	q_t (mg/g)	C_i (mg/L)	C_t (mg/L)	q_t (mg/g)	C_i (mg/L)	C_t (mg/L)	q_t (mg/g)
2	5.999	5.653	0.014	5.982	5.314	0.027	6.877	4.686	0.088
4	5.999	5.247	0.030	5.982	4.077	0.076	6.877	0.729	0.246
6	5.999	4.970	0.041	5.982	3.170	0.112	6.877	0.513	0.255
8	5.999	1.244	0.190	5.982	0.077	0.236	6.877	0.717	0.246
10	5.999	0.006	0.240	5.982	0.014	0.239	6.877	0.450	0.257

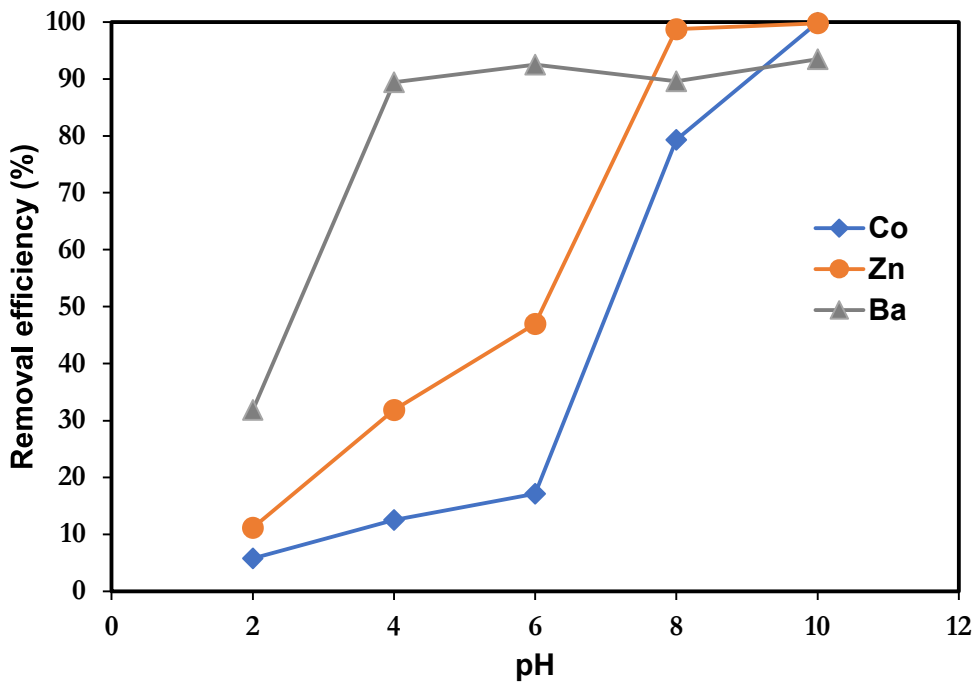

Figure 4.16: The variation of removal efficiency of Co, Zn and Ba ions with pH

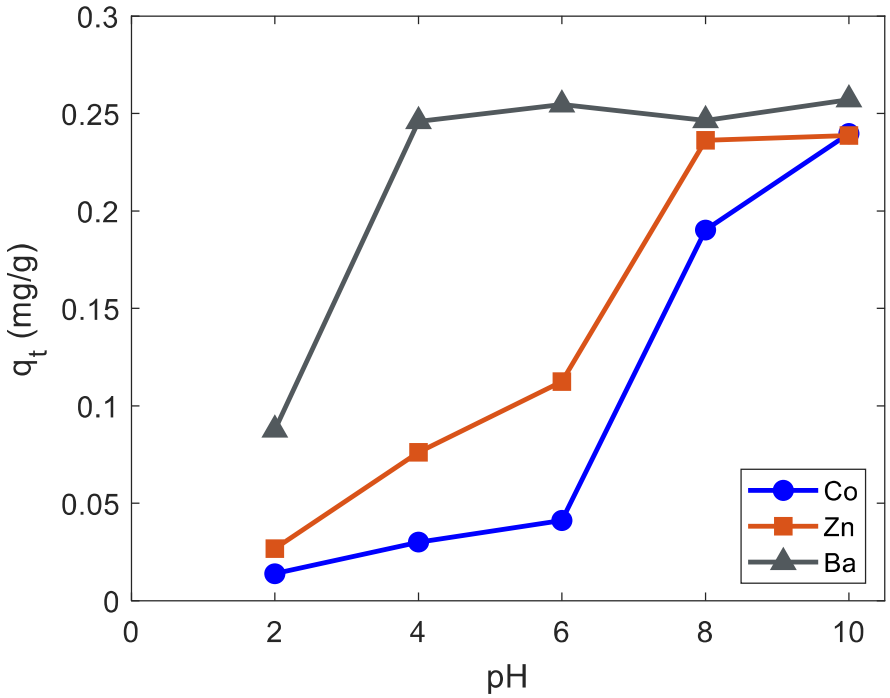

Figure 4.17: The variation of the amount of Co, Zn and Ba adsorbed on diatomite per unit mass of diatomite with the pH

CHAPTER 5: CONCLUSIONS AND RECOMMENDATIONS

5.1 Conclusions

a) In this study, Diatomite from Kariandusi mining area, has been characterized and its capacity for removal Ba, Co and Zn ions determined by equilibrating it with aqueous solution containing ions of Ba, Co and Zn.

b) The results of chemical and mineral phase characterization indicate that diatomite from Kariandusi is made of $91.64 \pm 2.99\,\%$ of silica in the form of cristobalite, in agreement with the expected composition of diatomite.

c) It was determined from the cation exchange capacity study that the diatomite sample from Kariandusi had a CEC of 7.94 ± 0.83 meq/100g, compared to the 9.8 meq/100g and 11.3 meq/100g obtained by Belousov et al (2019). The difference CEC value obtained in this study with those in the other studies can be attributed to the variation in the type and quantity of natural clays present in the diatomite.

d) Approximately, 10% of particles (d10) had diameter less than 171 µm; 50% of particles (d50) had a diameter of 589 µm; while 90% of particles (d90) were lesser than 1523 µm. Use of particle size distribution different from the one used in this study may affect the sorption efficiency due to the inverse relationship between particle size and sorption.

e) The results of the sorption with regard to removal of ions of Ba, Co and Zn were below the optimum sorption capacity. However, the removal efficiency of diatomite can be increased by increasing diatomite content, pH, contact time and/or decreasing the initial concentrations of Co, Zn and Ba.

f) Removal efficiency of up to 99% can be obtained with selection of the appropriate values of sorption parameters.

g) This study has indicated that diatomite has the capacity to adsorb Co (II), Zn (II) and Ba (II) ions from a general waste solution.

5.2 Recommendations

a) It is recommended that a study be conducted to determine the chemical and radiation stability of diatomite for the sorption of Co (II), Zn (II), and Ba (II) ions in their radioactive forms.

b) A study be conducted to determine the effect of particle size and pore size distribution on sorption of Co (II), Zn (II), Ba (II) ions and other ions typically present in liquid radioactive waste.

c) This report being on a study regarding removal of some species of heavy metal from aqueous solutions is an attempt to tackle an important and highly relevant contemporary problem. Furthermore, the proposed use of diatomite, a locally available and very abundant mineral, the study promises to develop an affordable and easy to apply method to achieve this. Whereas the study targeted only three heavy metals it is in fact highly likely that similar results could be achieved if other heavy metals are targeted instead. This was not done because of cost and logistical considerations, however, the results, with further testing, could find application in other situations as well.

REFERENCES

ADIL. (n.d.). *About Us*. African Diatomite. Retrieved March 21, 2021, from https://www.africandiatomite.com/index.php/about-us

Al-Degs, Y. (2001). Sorption of lead ions on diatomite and manganese oxides modified diatomite. *Water Research*, *35*(15), 3724–3728. https://doi.org/10.1016/s0043-1354(01)00071-9

Audero, M. A., Bevilacqua, A. M., de Bernasconi, N. B. M., Russo, D. O., & Sterba, M. E. (1995). Immobilization of simulated high-level waste in sintered glasses. *Journal of Nuclear Materials*, *223*(2), 151–156. https://doi.org/10.1016/0022-3115(94)00686-5

Aytaş, Ş., Akyil, S., Aslani, M. A. A., & Aytekin, U. (1999). Removal of uranium from aqueous solutions by diatomite (Kieselguhr). *Journal of Radioanalytical and Nuclear Chemistry*, *240*(3), 973–976. https://doi.org/10.1007/bf02349885

Bailey, S. E., Olin, T. J., Bricka, R. M., & Adrian, D. D. (1999). A review of potentially low-cost sorbents for heavy metals. *Water Research*, *33*(11), 2469–2479. https://doi.org/10.1016/s0043-1354(98)00475-8

Belousov, P., Semenkova, A., Egorova, T., Romanchuk, A., Zakusin, S., Dorzhieva, O., Tyupina, E., Izosimova, Y., Tolpeshta, I., Chernov, M., & Krupskaya, V. (2019). Cesium Sorption and Desorption on Glauconite, Bentonite, Zeolite and Diatomite. *Minerals*, *9*(10), 625. https://doi.org/10.3390/min9100625

Borges, V. F., de Oliveira, K. C., Braga, T. P., Fonseca, J. L. C., de Castro Dantas, T. N., & Wanderley Neto, A. O. (2019). Removal of metal cations by diatomite treated with microemulsion. *Journal of Dispersion Science and Technology*, *42*(2), 206–213. https://doi.org/10.1080/01932691.2019.1674153

Caliskan, N., Kul, A. R., Alkan, S., Sogut, E. G., & Alacabey, İ. (2011). Adsorption of Zinc(II) on diatomite and manganese-oxide-modified diatomite: A kinetic and equilibrium study. *Journal of Hazardous Materials*, *193*, 27–36. https://doi.org/10.1016/j.jhazmat.2011.06.058

ElSayed, E. (2018). Natural diatomite as an effective adsorbent for heavy metals in water and wastewater treatment (a batch study). *Water Science*, *32*(1), 32–43. https://doi.org/10.1016/j.wsj.2018.02.001

Flores-Cano, J. V., Leyva-Ramos, R., Padilla-Ortega, E., & Mendoza-Barron, J. (2013). Adsorption of Heavy Metals on Diatomite: Mechanism and Effect of Operating Variables. *Adsorption Science & Technology*, *31*(2–3), 275–291. https://doi.org/10.1260/0263-6174.31.2-3.275

Galal Mors, H. E. (2010). Diatomite: Its Characterization, Modifications and Applications. Asian Journal of Materials Science, 2(3), 121–136. https://doi.org/10.3923/ajmskr.2010.121.136

Giencke, J. (2007). *Introduction to EVA A Complete*. DOCPLAYER. https://docplayer.net/20207016-Introduction-to-eva-a-complete-orientation-to-features-and-functions-jonathan-giencke-application-engineer-x-ray-diffraction.html

IAEA. (1972). *Use of Local Minerals in the Treatment of Radioactive Waste* (1 3 6). http://www.iaea.org/inis/collection/NCLCollectionStore/_Public/04/059/4059411.pdf

IAEA. (1995). The Principles of radioactive waste management (Safety Series No. 111-S-1). Vienna (Austria): IAEA.

IAEA. (1997). Treatment technologies for low and intermediate level waste from nuclear applications (Final Report of a co-ordinated Research, TECDOC-929). Vienna(Austria): IAEA-International Atomic Energy Agency.

IAEA. (2003). Combined methods for liquid radioactive waste treatment (Final Report, TECDOC-1336). Viena (Austria): International Atomic Energy Agency.

Ibrahim, G. M. (2010). Removal of60Co and134Cs radionuclides from aqueous solution using titanium tungstate ion exchanger. *Desalination and Water Treatment*, *13*(1–3), 418–426. https://doi.org/10.5004/dwt.2010.999

Ibrahim, S. S., Ibrahim, H. S., Ammar, N. S., Abdel Ghafar, H. H., Jamil, T. S., & Farahat, M. (2013). Applicability of Egyptian diatomite for uptake of heavy metals. *Desalination and Water Treatment*, *51*(10–12), 2343–2350. https://doi.org/10.1080/19443994.2013.734581

Irani, M., Amjadi, M., & Mousavian, M. A. (2011). Comparative study of lead sorption onto natural perlite, dolomite and diatomite. *Chemical Engineering Journal*, *178*, 317–323. https://doi.org/10.1016/j.cej.2011.10.011

Isinkaye, M., & Ajayi, I. R. (2006). Natural background dose and radium equivalent measurements at Ikogosi warm spring, Nigeria. Radiation Protection Dosimetry, 121(4), 466–468. https://doi.org/10.1093/rpd/ncl065

Kim, J.-M., & Kim, C.-L. (2017). Performance Improvement of Liquid Waste Management System for APR1400. *Progress in Nuclear Energy*, *100*, 93–102. https://doi.org/10.1016/j.pnucene.2017.05.026

Kumar, P.S, Korving, L., Keesman, K. J., van Loosdrecht, M. C., & Witkamp, G. J. (2019). Effect of pore size distribution and particle size of porous metal oxides on phosphate adsorption capacity and kinetics. *Chemical Engineering Journal*, *358*, 160–169. https://doi.org/10.1016/j.cej.2018.09.202

Lu, S., Hu, J., Chen, C., Chen, X., Gong, Y., Sun, Y., & Tan, X. (2017). Spectroscopic and modeling investigation of efficient removal of U(VI) on a novel magnesium silicate/diatomite. *Separation and Purification Technology*, *174*, 425–431. https://doi.org/10.1016/j.seppur.2016.09.052

Mendioroz, S., Belzunce, M. J., & Pajares, J. A. (1989). Thermogravimetric study of diatomites. *Journal of Thermal Analysis*, *35*(7), 2097–2104. https://doi.org/10.1007/bf01911874

Meradi, H., Atoui, L., Ghabeche, W., & Bahloul, L. (2019). Contribution to Characterization of Natural Diatomite. *International Journal of Scientific Research & Engineering Technology (IJSET) Vol.9* pp.6-11. http://ipco-co.com/IJSET/vol9/issue-2/2.pdf

Mohamedbakr, H., & Burkitbaev, M. (2009). Elaboration and Characterization of Natural Diatomite in Aktyubinsk/Kazakhstan. *The Open Mineralogy Journal*, *3*(1), 12–16. https://doi.org/10.2174/1874456700903010012

Nattrass, C., Horwell, C. J., Damby, D. E., Kermanizadeh, A., Brown, D. M., & Stone, V. (2015). The global variability of diatomaceous earth toxicity: a physicochemical and in vitro investigation. Journal of Occupational Medicine and Toxicology, 10(1), 10–23. https://doi.org/10.1186/s12995-015-0064-7

Nenadovic, S., Kljajevic, L., Markovic, S., Omerasevic, M., Jovanovic, U., Andric, V., & Vukanac, I. (2015). Natural diatomite (Rudovci, Serbia) as adsorbent for removal Cs from radioactive waste liquids. *Science of Sintering*, *47*(3), 299–309. https://doi.org/10.2298/sos1503299n

Nenadovic, S., Nenadovic, M., Kovacevic, R., Matovic, L., Matovic, B., Jovanovic, Z., & Novakovic-Grbovic, J. (2009). Influence of diatomite microstructure on its adsorption capacity for Pb(II). *Science of Sintering*, *41*(3), 309–317. https://doi.org/10.2298/sos0903309n

Olatunji, M. A., Khandaker, M. U., & Mahmud, H. E. (2018). Adsorption kinetics, equilibrium and radiation effect studies of radioactive cesium by polymer-based adsorbent. Journal of Vinyl and Additive Technology, 24(4), 347-357.

Oliveira, E. (2003). Sample preparation for atomic spectroscopy: evolution and future trends. *Journal of the Brazilian Chemical Society*, *14*(2), 174–182. https://doi.org/10.1590/s0103-50532003000200004

Osmanlioglu, A. E. (2007). Natural diatomite process for removal of radioactivity from liquid waste. *Applied Radiation and Isotopes*, *65*(1), 17–20. https://doi.org/10.1016/j.apradiso.2006.08.012

Osmanlioglu, A. E. (2015). Immobilization of radioactive borate liquid waste using natural diatomite. *Desalination and Water Treatment*, *57*(32), 15146–15153. https://doi.org/10.1080/19443994.2015.1068225

Otwoma, D., Patel, J. P., Bartilol, S., & Mustapha, A. O. (2012). Radioactivity And Dose Assessment of Rock and Soil Samples From Homa Mountain, Homa Bay County, Kenya. In Radiation Physics & Protection Conference (XI). IAEA. https://inis.iaea.org/collection/NCLCollectionStore/_Public/45/099/45099897.pdf

Piri, M., Sepehr, E., Samadi, A., Farhadi, K. H., & Alizadeh, M. (2020). Contaminated soil amendment by diatomite: chemical fractions of zinc, lead, copper and cadmium. *International Journal of Environmental Science and Technology*. https://doi.org/10.1007/s13762-020-02872-0

Rahman, R. O. A., Ibrahium, H. A., & Hung, Y.-T. (2011). Liquid Radioactive Wastes Treatment: A Review. *Water*, *3*(2), 551–565. https://doi.org/10.3390/w3020551

Saint-Fort, R. (2018). Understanding sorption behavior and properties of radionuclides in the environment. *Principles and applications in nuclear engineering: radiation effects, thermal hydraulics, radionuclide migration in the environment*, *121*(1).

Salman T., Temel F.A., Turan N.G. and Ardali Y. (2016), Adsorption of lead (II) ions onto diatomite from aqueous solutions: mechanism, isotherm and kinetic studies. *Global NEST Journal, 18(1)*, 1-10. https://doi.org/10.30955/gnj.001564

Sandhya, K., Prakash, N. B., & Meunier, J. D. (2018). Diatomaceous earth as source of silicon on the growth and yield of rice in contrasted soils of Southern India. *Journal of Soil Science and Plant Nutrition*, *ahead*, 0. https://doi.org/10.4067/s0718-95162018005001201

Shareef, K. M. (2009). Sorbents for Contaminants Uptake from Aqueous Solutions. *World Journal of Agricultural Sciences (S)*, 819-831.

Sheng, G., Dong, H., & Li, Y. (2012). Characterization of diatomite and its application for the retention of radiocobalt: role of environmental parameters. *Journal of Environmental Radioactivity*, *113*, 108–115. https://doi.org/10.1016/j.jenvrad.2012.05.011

Sheng, G., Hu, J., & Wang, X. (2008a). Sorption properties of Th (IV) on the raw diatomite—Effects of contact time, pH, ionic strength and temperature. *Applied Radiation and Isotopes*, *66*(10), 1313–1320. https://doi.org/10.1016/j.apradiso.2008.03.005

Sheng, G., Hu, J., & Wang, X. (2008b). Sorption properties of Th (IV) on the raw diatomite—Effects of contact time, pH, ionic strength and temperature. *Applied Radiation and Isotopes*, *66*(10), 1313–1320. https://doi.org/10.1016/j.apradiso.2008.03.005

EPA (2020, July 9) SW-846 Test Method 9081: Cation-Exchange Capacity of Soils (Sodium Acetate). https://www.epa.gov/hw-sw846/sw-846-test-method-9081-cation-exchange-capacity-soils-sodium-acetate

WAC. (2014). Method for Analysing Soil Samples for Mineral Composition Using XRD. Standard Operating Procedures (laboratory manual prepared by World Agroforestry Center). World Agroforestry Center.

WU, J., YANG, Y., & LIN, J. (2005). Advanced tertiary treatment of municipal wastewater using raw and modified diatomite. *Journal of Hazardous Materials*, *127*(1–3), 196–203. https://doi.org/10.1016/j.jhazmat.2005.07.016

Yusan, S., Gok, C., Erenturk, S., & Aytas, S. (2012). Adsorptive removal of thorium (IV) using calcined and flux calcined diatomite from Turkey: Evaluation of equilibrium, kinetic and thermodynamic data. *Applied Clay Science*, *67–68*, 106–116. https://doi.org/10.1016/j.clay.2012.05.012

Zhang, X., Gu, P., & Liu, Y. (2019). Decontamination of radioactive wastewater: State of the art and challenges forward. *Chemosphere*, *215*, 543–553. https://doi.org/10.1016/j.chemosphere.2018.10.029